Université de Montréal

Azacyclopeptide synthesis and their neuroprotective activity against Aβ toxicity

Par

Suresh Vutla

Département de chimie

Faculté de arts et des sciences

Mémoire présenté à la Faculté des études supérieures et postdoctorales

en vue de l'obtention du grade de

maître ès sciences (M.Sc.)

en chimie

August 2018

Résumé:

Le mauvais repliement et l'agrégation des protéines représentent une cause fondamentale des pathologies amyloïdes. Des dépôts de protéines sous la forme de fibrilles amyloïdes sont une composante caractéristique de plus de vingt maladies neurodégénératives incluant la maladie d'Alzheimer, la maladie de Parkinson et la maladie d'Huntington. Des nanotubes composés de peptides-α-D,L cycliques synthétiques peuvent mimer les propriétés structurelles et biochimiques des protéines amyloïdes. L'introduction de résidus aza-aminés dans des peptides α-D,L cycliques a été étudiée dans le but d'augmenter les interactions hydrogènes intermoléculaires entre les différents macrocycles superposés composant le nanotube. Les peptides aza-α-D,L cycliques devraient aussi posséder une meilleure capacité d'interaction avec les feuillets des oligomères amyloïdes.

Le peptide d'intérêt **CP-2** possède la séquence [l-J-w-H-s-K], où les lettres minuscules et majuscules font référence respectivement aux acides aminés D et L, les crochets indiquent une structure cyclique et la lettre « J » représente la norleucine. En exploitant la capacité des semicarbazides d'accroitre les ponts hydrogènes intermoléculaires, nous avons remplacés successivement chacun des acides aminés de la séquence **CP-2** par un résidu aza-glycine, obtenant une librairie d'azapeptides cycliques. Ces peptides ont été testés pour leur propriété neuroprotectrice contre les amyloïdes β en utilisant un essai de viabilité cellulaire (essai MTT). Le peptide où la D-serine a été remplacée par une aza-glycine, **CP-2 (4)**, s'est avéré plus efficace que **CP-2**. Il s'agit du premier exemple d'introduction d'un résidu aza-aminé dans un peptide α-D,L cyclique, et ces résultats pourraient être extrapolés à d'autres peptides α-D,L cycliques d'intérêt thérapeutique.

Mots-clés : Amyloïde, Maladie d'Alzheimer, Peptides α-D,L cycliques, Structures tubulaires, Azapeptides

Abstract:

Protein misfolding and aggregation are the fundamental causes of amyloid diseases. Deposits of proteins in the form of amyloid fibrils and plaques are the characteristic features of more than twenty degenerative conditions, including Alzheimer's, Parkinson's, and Huntington's diseases. Synthetic cyclic D,L-α-peptide nanotubes can mimic the structural and biochemical properties of amyloid proteins. The introduction of aza-residues into cyclic D,L-α-peptides was studied to enhance intermolecular hydrogen bonding between stacked rings within the tube structures. The resulting cyclic aza-D,L-α-peptides were also expected to exhibit enhanced propensity to interact with the sheet structures of amyloid oligomers.

The lead peptide **CP-2** features the sequence [l-J-w-H-s-K] in which lower and upper-case letters indicate D- and L-amino acids, respectively, square brackets designate a cyclic structure, and J denotes norleucine. There are no reports for introduction of aza-residues into cyclic D,L-α-peptides. Considering the potential for semicarbazides to enhance intermolecular hydrogen bonding, we performed an aza-glycine scan of the **CP-2** sequence by preparing a focused library of azapeptides. All the cyclic aza-glycine peptides were tested for neuroprotective activity against amyloid β using cell viability assay (MTT assay). The aza-glycine replacing D-serine i.e., [azaG^2]-**CP-2 (4)** was found to be more potent than **CP-2**. This is the first example of introducing an aza-amino residue into a cyclic D, L-α- peptide, and these results could be extrapolated to other cyclic D, L-α-peptides of therapeutic interest.

Key words: Amyloid, Alzheimer's disease, Cyclic D,L-α-peptides, Tubular structures, Azapeptides

Table of Contents:

Contents

List of Figures

List of Schemes

List of Tables

List of Abbreviations

μ	Micro
Aβ	Amyloid β
Ach	Acetylcholine
AChE	Acetylcholinesterase Enzyme
AcOH	Acetic acid
AD	Alzheimer's disease
APP	Amyloid precursor protein
BBB	Blood brain barrier
br	Broad (in NMR)
CDI	1,1'-Carbonyldiimidazole
CSF	Cerebrospinal fluid
CT	Computed Tomography
d	Doublet (in NMR)
dd	Doublet of doublets (in NMR)
DCM	Dichloromethane
Dde	1-(4,4-Dimethyl-2,6- dioxocyclohexylidene)-3-methylbutyl-
DIC	*N,N'*-Diisopropylcarbodiimide
DIPEA	*N,N*-Diisopropylethylamine
Dmab	4-{*N*-[1-(4,4-dimethyl-2,6-dioxocyclohexylidene)-3-methylbutyl]amino}benzyl-
DMF	*N,N*-Dimethylformamide
DMSO	Dimethyl sulfoxide
DSC	*N,N'*-Disuccinimidyl carbonate
EDC•HCl	1-Ethyl-3-(3-dimethylaminopropyl)carbodiimide hydrochloride
ESI+	Electrospray ionization mode positive mode
ES-MS	Electrospray mass spectrometry
EtOAc	Ethyl acetate
FDA	Food and Drug Administration

FDG	Fluorodeoxyglucose
HIV	Human immunodeficiency virus
HOBt	Hydroxybenzotriazole
HPLC	High-performance liquid chromatography
HRMS	High resolution mass spectrometry
IgG	Immunoglobulin G
J	Coupling constant (in NMR)
LC/MSD	Liquid Chromatography/Mass Selective Detector
LHRH	Luteinizing hormone-releasing hormone
m	Multiplet (in NMR)
mAbs	Monoclonal antibodies
MHz	Megahertz (in NMR)
MRI	Magnetic Resonance Imaging
MTT	3-(4,5-dimethylthiazol-2-yl)-2,5-diphenyltetrazolium bromide
NMDA	*N*-methyl-D-aspartate
NMP	*N*-Methyl-2-pyrrolidone
NMR	Nuclear magnetic resonance
PBS	Phosphate-buffered saline
PC12	Pheochromocytoma
PET	Positron Emission Tomography
PPM	Parts per million (in NMR)
s	Singlet (in NMR)
SPPS	Solid phase peptide synthesis
t	Triplet (in NMR)
TES	Triethyl silane
TFA	Trifluoroacetic acid
TFE	2,2,2-Trifluoroethanol
THF	Tetrahydrofuran

TLC	Thin layer chromatography
UV	Ultraviolet
VHH	Heavy chain variable domain

Acknowledgments

First and foremost, I would like to thank graciously my supervisor, Professor William D. Lubell for giving me the opportunity to improve my knowledge in the field of chemistry. Professor Lubell supported me throughout my thesis with his patience and suggested thoughtful comments.

I kindly thank to Dr. Shai Rahimipour and his laboratory personnel for analysing the biological activity of the analogues and for providing the results to include in my thesis.

I acknowledge to the Department of Chemistry, Université de Montréal for providing facilities and admission to peruse my study. I would like to thank all my group members for providing me the support during my study and work.

I would like to thank Dr. Alexandra Furtos-Matei, Karine Gilbert, Marie-Christine Tang, Simon Comtoi-Marotte and Louiza Mahrouche from the Mass Spectrometry Centre for assistance with HRMS and LCMS analyses; Pedro Aguiar, Sylvie Bilodeau, Antoine Hamel and Cedric Malveau from the NMR Spectroscopy Centre for help with NMR analyses.

I would like to thank my family, especially my loving parents, spouse, sisters and child for their endless support. I am grateful to all who supported me to come to Montreal to pursue my M.Sc. studies.

Chapter 1: Introduction

1.1. Alzheimer's disease, an amyloid protein-caused healthcare concern

Amyloidosis is abnormal protein accumulation in body tissues and organs characteristic of amyloid diseases. Amyloid was first considered a starch-like substance because of a positive iodine staining reaction,[1-4] characteristic of the amylaceous component in plants. Subsequently, interactions with other dyes indicated amyloid was indeed a protein and not a carbohydrate.[1]

Contingent on the type of amyloid, amyloidosis can have life threatening affects on the shape and functions of various organs: heart, liver, spleen, kidneys and the nervous system. Dementia with impaired memory and thinking is characteristic of many amyloid neurodegenerative diseases, among which Alzheimer's disease (AD) is the most common and responsible for about 60-80% of all cases.[5] Predominantly affecting the elderly, without effective therapy, the frequency of Alzheimer's disease is expected to parallel the aging worldwide population and grow from 10.6 to 13.8 million over the period between 2016-2026.[6-7] Alzheimer's disease is a major worldwide healthcare and economic burden. In the United States alone, the total projected cost for Alzheimer's disease is estimated to be $US 277 billion for 2018, and expected to grow by a factor of four to $US 1.1 trillion by 2050.[8] In 2017, life-time costs for a single Alzheimer's disease patient were estimated to be $US 341,840.

1.2. Diagnostics for Alzheimer's disease

1.2.1. Diagnostics are needed for early detection of Alzheimer's disease

Early diagnosis may open opportunity for better care and treatment, provide savings for long-term care,[9] and improve quality of life.[10] Early detection may improve access to normal brain function and potential to delay institutionalization by using disease modifying therapies and available drugs that can treat mild to moderate AD.[11] Overall, early detection may provide a means to reduce the socio-economic costs of AD.

1.2.2. Current diagnostics for Alzheimer's disease

Presently, no single test exists to identify AD. Symptoms such as loss of memory and mental ability may lead a physician to test blood and vision, prior to using computed tomography (CT) and magnetic resonance imaging (MRI) scans.[12-15] In a CT scan, several X-rays of the brain are record at different angles and assembled to identify tumors and plaques that may cause memory loss.[16] More detailed images of the brain may be recorded by MRI, which uses radio waves within a strong magnetic field to influence the naturally abundant nuclei such as the protons in water.[17] Brain abnormalities related to mild cognitive impairment and Alzheimer's disease may be distinguished by MRI.[18] Over time, MRI of Alzheimer's disease patients can detect the decreasing size of different areas of the brain.[19] Both CT and MRI are mainly used to exclude other possible causes for dementia such as tumors and abnormalities in brain, vascular and inflammatory systems.[20] MRI can be used to estimate tissue damage and defected brain regions during AD. Additionally, MRI can differentiate AD from other neurodegenerative disease. MRI is more reliable over CT to identify early signs related to AD.[21] Brain Positron Emission Tomography (PET) is also test used to diagnose AD, by measuring metabolic and molecular changes of the brain. With potential to provide detailed 3-dimensional images of organs and abnormal tissue, PET can assess the severity of disease. PET is more sensitive than MRI for detecting pathologies on the molecular level in early diagnoses.[22] Notably, PET and MRI scans may be combined to improve imaging accuracy.

In spite such techniques, accurate diagnosis of AD is still difficult especially in early stages. The use of biomarkers (e.g., radio tracers) is being pursued to identify early stages of AD. Currently two imaging markers are being used to study AD: cerebrospinal fluid (CSF) is detectable by MRI,[21] the persons with mild cognitive impairment (MCI) having low CSF Aβ42 levels is an

indicative for the presence of early AD[23-24] and ^{18}F- fluorodeoxyglucose (^{18}F-FDG) is used to diagnose neuronal function by PET imaging of regional glucose metabolism, which is associated with high cost, limited availability and inconsistent results.[25-26]

Disease specific protein biomarkers such as immunoglobulin G antibodies (IgGs) are abundant in accessible biological fluids, such as cerebral spinal fluid (CSF) and human blood serum, and influenced by age, gender and diseases.[27] Amplification of IgG antibodies may be due to disease-specific antigens, and used to assess the pathology of neurogenerative diseases, such as AD.[24, 28-29] The major disadvantage in acquiring CSF is lumbar spinal puncture associated with invasive pain and risk.[30]

The development of biomarkers for AD brain lesions has focused on ligands useful for PET imaging.[31-32] Drawbacks include the requirement to cross the blood-brain barrier (BBB) of central nervous system which may require opening by ultrasound[33-34] or permeability enhancers such as mannitol.[35] The development of homo-dimeric heavy chain antibodies which can cross the BBB after peripheral injection may circumvent such aggressive and dangerous procedures.[36,37] The antibodies, which have only the heavy chain variable domain, can facilitate interaction with the intracellular target and visualization of intracellular brain targets in AD.[38-39] With capacity to penetrate the brain more efficiently than conventional IgGs, such antibodies may be conjugated with gadolinium to provide a novel *in vivo* MR imaging agents for AD.[40]

1.3. Current treatment for Alzheimer's disease

There is no medication available to cure or slowdown neuronal damage by Alzheimer's disease. The U.S. Food and Drug Administration (FDA) has approved five drugs so far for the treatment of mild to moderate Alzheimer's disease: tacrine (1993), donepezil (1996), rivastigmine

(1998), galantamine (2001) and memantine (2003).[41] The first four drugs inhibit the enzyme acetylcholinesterase (AChE) to impair hydrolysis and to increase availability of acetylcholine (Ach). A neurotransmitter, Ach is a chemical involved in brain communication (cholinergic function). The brain of AD patients have low Ach levels, which correlates with accumulation of the amyloid protein Aβ.[42] Memantine is an *N*-methyl-D-aspartate (NMDA) receptor antagonist, that regulates glutamate excitotoxicity and neurodegeneration,[43] by mitigating neuronal damage caused by excess glutamate in AD patients.[44]

The above drugs may improve symptoms temporarily by increasing neurotransmitters in brain. Cholinesterase inhibitors can stabilize symptoms between 1 and 2 years without modifying progression of the disease, as evidenced in clinical trials,[45] but effectiveness and efficiency vary from person to person.

In recent years, alternative approaches (i.e., anti-amyloid strategies) have been pursued for treating AD. For example, attempts to reduce the production of Aβ have employed β- and γ-secretase inhibitors, and to enhance the clearance of neurotoxic amyloid β, monoclonal antibodies have been employed.[46] Misprocessing of amyloid precursor protein (APP) by β- and γ-secretase enzymes causes accumulation of toxic Aβ in the brain.[47] Success in using β- and γ-secretase inhibitors to target the metabolic path that produces Aβ remains however ambiguous.[48]

Enhancing clearance of Aβ is another anti-Aβ immunotherapy involving passive and active immunization. Passive immunization is performed by administering exogenous anti-Aβ monoclonal antibodies (mAbs) like bapineuzumab and solanezumab to boost resistance to the aggregation of amyloid beta and help the immune system to remove amyloid already aggregated into plaques.[49] Several mAbs are currently being explored in clinical trials.[50]

Active immunization using vaccines containing fragments of amyloid beta and related antigens is used to stimulate the patient's immune system to produce its own antibodies.[51] An AD vaccine (CAD106), which targets antibody production against the Aβ 1-6 amino acid peptide fragment has advanced to phase III clinical trials.[51] Applications of mAbs and vaccines have however yet to prove successful and remain in the developmental stages.[50]

1.4. Cyclic peptides

Cyclic peptides can enhance conformational rigidity, bioavailability, potency, selectivity and binding affinity.[52-54] Compared to their linear counterparts, cyclic peptides may decrease the entropy for folding and improve receptor affinity.[53-55] The cyclic structure can facilitate resistance to enzymatic hydrolysis due to the lack of amine and carboxylic acid termini and conformational rigidity.[55] Certain cyclic peptides may stack to create supramolecular structures through intermolecular hydrogen-bonding,[56] such as nanotubes with potential biomedical applications.[54, 57]

1.4.1. Synthesis of Cyclic peptides

Various synthetic methodologies have been used to make cyclic peptides including amide and disulfide formation, copper-catalyzed azide-alkyne cycloadditions, and olefin metathesis.[58-60] In principle, cyclic peptides can be obtained via four different type of cyclization: head-to-tail, head-to-side chain, tail-to-side chain and side chain-to-side chain (Figure 1).[61-62] Head-to-tail cyclization entails peptide bond formation between *N*- and C-terminal amine and carboxylate groups.[58]

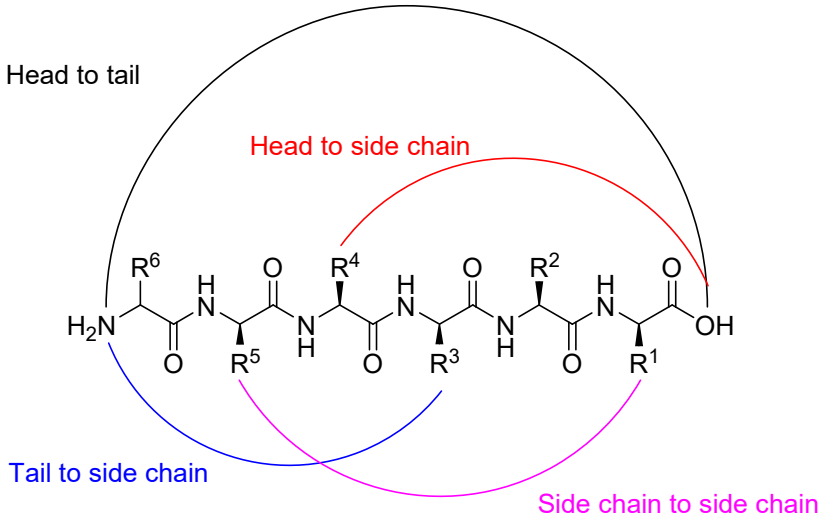

Figure 1.1: Possible pathways for peptide macrocyclization

Macrocyclization reactions in solution are usually performed at high dilution to avoid intermolecular side reactions.[58] Controlled mixing,[63] pseudo-dilution on solid phase,[64] and other methods[65-66] have been employed to favor cyclization at higher concentrations. In the solid-phase synthetic strategy, orthogonal protecting groups must be employed to mask the reactive components of the linear peptide prior to cyclization on-resin.[61, 67] The resin linkage and the side-chain protection must be compatible with common protecting group strategies (e.g., Boc and Fmoc) for the synthesis of the sequence backbone, but selectively removable to enable macrocyclization.[68] For example, Alloc and Dmab groups have been respectively used for orthogonal protection of amine and acid functions during sequence elongation using Boc and Fmoc chemistry and selectively cleaved prior to macrocyclization.[69-70]

1.5. Cyclic D,L-α-Peptides

Tubular structures have diverse applications in a variety of scientific fields including chemistry, biology, materials science and nontechnology.[57, 71-81] Cyclic D,L-α-peptides are a class of cyclic peptides that form tubular supramolecular structures by self-assembly through hydrogen-

bond directed ring stacking (Figure 1.1).[56, 82] Linear α-peptides possessing all L-amino acids exhibit generally sinusoidal backbone confirmations.[82-83] Systematic alternation of neighbouring amino acid configuration causes typically steric interactions that favour turn and helical conformations.[83-85] In a cyclic peptide, such alternation of neighbouring amino acid configuration positions the backbone amide hydrogen donors (NH) and acceptors (C=O) in an orientation suitable for forming intermolecular hydrogen bonds that favour aggregation of β-sheet-like nanotubes.[56]

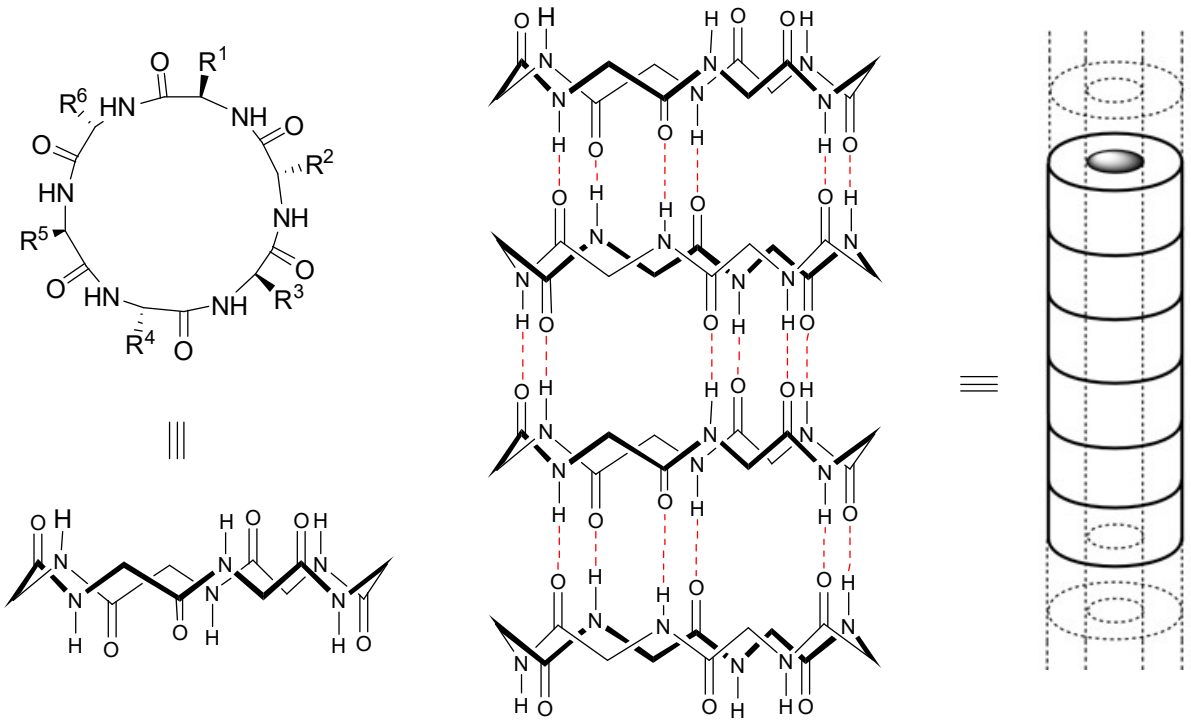

Figure 1.2: Cyclic D,L-α-peptides self- assemble through hydrogen-bonding interactions to form cylindrical structures

The Aβ peptide aggregates as β-sheets in the amyloid fibers, which exhibit structural complementarity to cyclic D,L-α-peptides.[86] Amyloidogenic proteins, such as Aβ, can interact with cyclic D,L-α-peptides to form supramolecular structures which may modulate aggregation.[87]

For example, anti-amyloidogenic activity has been exhibited by cyclic D,L-α-peptide hexamers, such as *c*-[lLwHsK] (**CP-1**, capital and small letters indicate L- and D-amino acids respectively).[87] Replacement of L-leucine by L-norleucine (Nle, J) gave an analogue (**CP-2**, *c*-[lJwHsK]) exhibiting superior activity compared to **CP-1** (Figure 1.2).[87-88] For example, **CP-2** interacted strongly and inhibited Aβ aggregation in Transmission Electron Microscopy (TEM) analyses, thioflavin T aggregation assays and cell survival studies.[87-88]

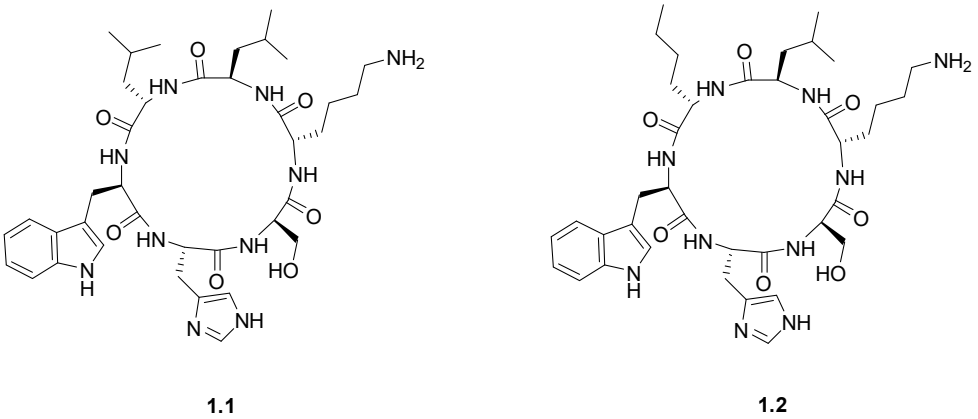

Figure 1.3: Structures of **CP-1 (1)** and **CP-2 (2)**

A series of single residue replacements with other amino acids were performed to examine the importance of each amino acid residue in the sequence of **CP-2** for biological activity.[88] For example, the significance of the aromatic and hydrophobic interactions of D-Trp and D-Leu for anti-amyloid forming activity were shown by replacement with D-Ala, which produced cyclic peptides having lower anti-amyloid activity. Attempts to augment the hydrophobic interactions of Nle by replacement with 2-aminooctanoic acid and cyclohexylalanine failed to increase anti-amyloid activity, but replacement of Nle by Phe enhanced potency against Aβ aggregation.[88] On the other hand, replacement of His, D-Ser and Lys by L- or D-Ala respectively caused little influence on activity.

1.6. Aza-peptides

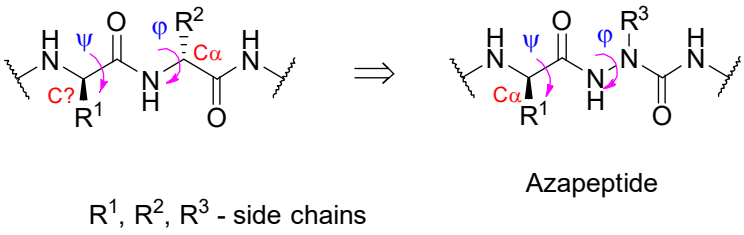

Figure 1.4: General structure for azapeptide

Azapeptides are a class of modified peptides in which the backbone α-carbon of one or more amino acid is replaced with nitrogen (Figure 1.3).[89-93] The resulting modification in which an amino amide is replaced by a semicarbazide makes the backbone more rigid due to urea planarity and electronic repulsion of lone pairs of the adjacent nitrogen.[91, 94-98] Chirality about the α-center may shift from the tetrahedral carbon geometry to a potentially dynamic nitrogen that can adopt both planar sp^2 and tetrahedral sp^3 hybridization. Azapeptides have been shown to adopt the central residues of β-turn conformations.[91, 94-99] Moreover, relative to a peptide amide, the α-nitrogen increases the acidity of the neighbouring acyl nitrogen NH, which may augment capacity to form hydrogen bonds.[91] In addition, substitution with aza-glycine results in the potential for an additional hydrogen bond donor.

Since aza-valine was introduced into bovine angiotensin II (H-Asp-Arg-azaVal-Tyr-Val-His-Pro-Phe-OH) by the Pfizer group and showed reduced activity but longer duration of action than the parent peptide,[100] aza-amino acids have been successfully introduced into various peptide hormones,[91, 100] and a number of different peptide-based protease inhibitors.[101-102] In clinic, the aza-glycinamide analog of LHRH known as Zoladex™ is currently used to treat soft tissue cancers.[103-105] Atazanavir™ is an aza-peptide mimic protease inhibitor used in anti-retroviral therapy against HIV.[106-108]

1.6.1. Synthesis of Azapeptides

Azapeptides feature peptide backbone amino acid residues in which the α-carbon is replaced with nitrogen. Several methods have been used to introduce aza-amino acids into linear peptides to make azapeptides in solution and on solid-support (Scheme 1).[89] The aza-residue can be introduced by activating the *N*-terminus of an amino acid residue with a carbonyl donor which is reacted with a hydrazine moiety (Path I).[13-14] Carbonyl donors can be introduced using triphosgene[17]or carbonic anhydrides;[109-111] however, a disadvantage of this strategy is the formation of hydantoin from intramolecular nucleophilic attack by the *C*-terminal amide nitrogen. Reversible amide protection with *N*-2-hydroxy-4-methoxybenzyl (Hmb) has avoided hydantoin at the cost of two additional synthetic steps.[112] In a second approach (Path II), activated aza-amino acid analogs are coupled to the terminal amino acid residue. Activation can be achieved by treating hydrazine analogs with various coupling reagents, such as triphosgene,[113-114] phosgene,[95, 115-116] carbonyl diimidazole (CDI)[117-119] and *N,N′*-disuccinimidyl carbonate (DSC).[120-121] A drawback that is especially observed in the case of aza-glycine residues is intramolecular cyclization to form oxadiazalone side product from the activated intermediate. The employment of hydrazone and semicarbazone intermediates has avoided oxadiazalone formation during aza-glycine installation.[122-123] Once the aza residue is installed into the peptide back bone, the final azapeptide may be synthesized by standard solid phase peptide synthesis (SPPS). In the sub-monomer approach to azapeptides (Path III), aza-glycine peptides are synthesized by hydrazine activation as a methylidene carbazate and coupled to the *N*-terminal amino acid residue. Subsequently, the azapeptide is produced by alkylation of the resulting semicarbazone, selective liberation of the corresponding semicarbazide and sequence elongation. The advantages of the latter strategy

include the suppression of intramolecular cyclized biproducts and the potential to introduce a variety of side chains onto the aza-glycine residue.

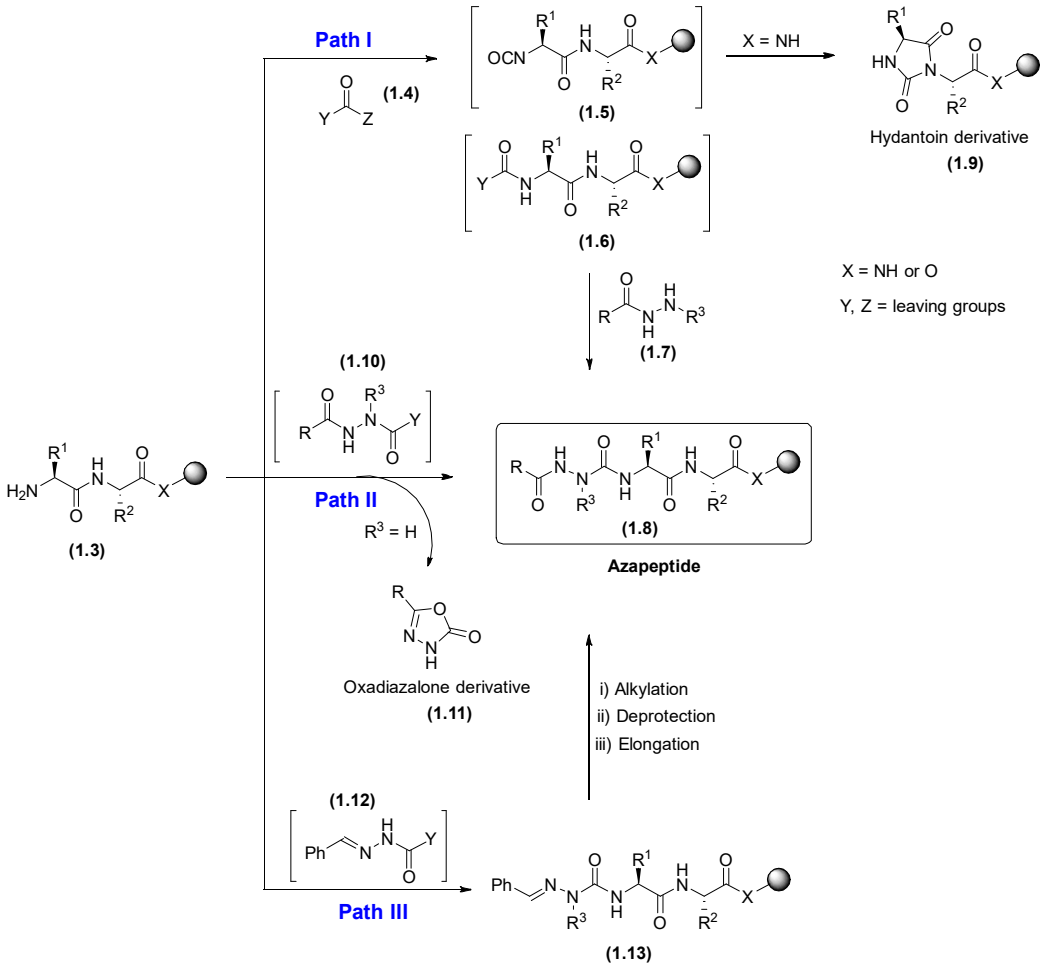

Figure 1.5: Possible pathways for synthesis of azapeptides.

1.7. Aza-glycine peptides

According to computational analysis, aza-glycine has greater conformational liberty than substituted aza-amino acids.[124] Aza-glycine may induce a bent structure, with a 90° twist about the N-N torsion angle. Aza-glycine has replaced glycine in several active peptides. For example, aza-glycine analogues of oxytocin,[125] and Arg-Gly-Asp (RGD)-containing antagonists of the integrin

receptors have shown greater activity.[115-116, 126-128] Moreover, [Aza Gly^{33}]-CGRP exhibited 10-fold greater antagonism potency than its parent glycine peptide counterpart.[129]

Collagen backbone modification has revealed the importance of maximizing hydrogen bonding to stabilize the triple helical structure.[130-131] Replacement of glycine by aza-glycine in the collagen triple helix incorporated an extra hydrogen bonding unit that stabilized the coiled-coiled structure.[130-131] Collagen model peptide was analyzed using molecular dynamics to know the hydrogen bonding paramater in triple helix structure. This analysis revealed that azaG residue having posibilty to get three nonbonding interaction and the newly introduced α-Nitrogen is participating in two hydrogen bonding interactions.

The improved activity of aza-Gly analogs bodes well for applications of this residue in other peptides. In particular, potential to improve hydrogen bonding suggests that introduction of aza-Gly into cyclic D,L-α-peptides may enhance self-aggregation as well as association with soluble Aβ fibrils.

1.8. Aim of the project

The main goal of this project is to synthesize aza-glycine analogues of **CP-2** in which each amino acid residue is sequentially replaced by aza-glycine. The resulting analogues will be tested for anti-amyloidogenic activity using the Thioflavin T (ThT) assay, as well as neuroprotective activity in a cell viability assay (MTT assay). Biological assessment of the aza-glycine cyclic peptides was performed to provide insight into their aggregation propensity and association with soluble Aβ fibrils.

The cyclic peptide **CP-2** was selected for this study due to promising anti-amyloid and neuroprotective biological activity.[87-88] Introduction of aza-glycine residues into the peptide

backbone was pursued to exam potential to enhance self-assembly by enhancing hydrogen bonding capacity due to the replacement of the α-carbon with a more electronegative nitrogen atom and an additional hydrogen-bond donor.

The synthesis of **CP-2** has been previously performed by elongation of a linear peptide lJwHsK in which the L-lysine ε-amine is anchored onto the solid-support. Final cyclization was performed on resin by coupling the carboxylate of L-lysine onto the amine of D-leucine. Our initial plan was to synthesize all six analogues of **CP-2** by using a similar method in which each amino acid residue is systematically replaced with aza-glycine. Head-to-tail cyclization of the linear peptide terminating with a less nucleophilic semicarbazide residue was however anticipated to be a challenge, and avoided by an alternative approach featuring synthesis of linear azapeptides on solid phase and cyclization in solution.

1.9. References

1. Sipe, J. D.; Cohen, A. S. History of the amyloid fibril. *J. Struct. Biol.* **2000,** *130*, 88-98.

2. Kyle, R. A. Amyloidosis: a convoluted story. *Br. J. Haematol.* **2001,** *114*, 529-538.

3. Fändrich, M. On the structural definition of amyloid fibrils and other polypeptide aggregates. *Cell. Mol. Life Sci.* **2007,** *64*, 2066-2078.

4. Kisilevsky, R.; Raimondi, S.; Bellotti, V. Historical and current concepts of fibrillogenesis and in vivo amyloidogenesis: Implications of amyloid tissue targeting. *Front. Mol. Biosci.* **2016,** *3*, 17.

5. Frozza, R. L.; Lourenco, M. V.; De Felice, F. G. Challenges for Alzheimer's disease therapy: Insights from novel mechanisms beyond memory defects. *Front. Neurosci.* **2018,** *12*, 37.

6. Thies, W. B., L. 2013 Alzheimer's disease facts and figures. *Alzheimer's & Dementia* **2013,** *9*, 208-245.

7. Neeti Sharma, A. N. S. Exploring Biomarkers for Alzheimer's Disease. *J. Clin. Diagn. Res.* **2016,** *10*, KE01-KE06.

8. Gaugler;, J.; James;, B.; Johnson;, T.; Marin;, A.; Weuve, J. 2018 Alzheimer's disease facts and figures. *Alzheimer's & Dementia: The Journal of the Alzheimer's Association* **2018,** *14*, 367-429.

9. Mcainey, C. A.; Harvey, D.; Schulz, M. E. First Link: strengthening primary care partnerships for dementia support. *Can. J. Commun. Ment. Health* **2009,** *27*, 117-127.

10. Leifer, B. P. Early diagnosis of Alzheimer's disease: clinical and economic benefits. *J. Am. Geriatr. Soc.* **2003,** *51*, S281-S288.

11. Sharma, N.; Singh, A. N. Exploring biomarkers for Alzheimer's disease. *J. Clin. Diagn. Res.* **2016,** *10*, KE01.

12. McKhann, G.; Drachman, D.; Folstein, M.; Katzman, R.; Price, D.; Stadlan, E. M. Clinical diagnosis of Alzheimer's disease: Report of the NINCDS—ADRDA Work Group under the

auspices of Department of Health and Human Services Task Force on Alzheimer's Disease. *Neurology* **2011,** *77*, 333-333.

13. Xanthakos, S.; Krishnan, K. R. R.; Kim, D. M.; Charles, H. C. Magnetic resonance imaging of Alzheimer's disease. *Prog. Neuro-Psychopharmacol. Biol. Psychiatry* **1996,** *20*, 597-626.

14. Tokuchi, R.; Hishikawa, N.; Sato, K.; Hatanaka, N.; Fukui, Y.; Takemoto, M.; Ohta, Y.; Yamashita, T.; Abe, K. Differences between the behavioral and psychological symptoms of Alzheimer's disease and Parkinson's disease. *J. Neurol. Sci.* **2016,** *369*, 278-282.

15. Bandelow, S.; Clifford, A.; van der Wardt, V.; Hogervorst, E.; Madden, M.; Lindesay, J.; Gale, A. Accurate non-invasive diagnoses of Alzheimer's disease using eye scanning. *Alzheimer's & Dementia* **2011,** *7*, S155-S156.

16. Burns, A. BRAIN IMAGING: Computed tomography in Alzheimer's disease. *Lancet* **1993,** *341*, 601-602.

17. Berger, A. Magnetic resonance imaging. *BMJ* **2002,** *324*, 35-35.

18. Lehéricy, S.; Marjanska, M.; Mesrob, L.; Sarazin, M.; Kinkingnehun, S. Magnetic resonance imaging of Alzheimer’s disease. *Eur. Radiol.* **2007,** *17*, 347-362.

19. Johnson, K. A.; Fox, N. C.; Sperling, R. A.; Klunk, W. E. Brain Imaging in Alzheimer Disease. *Cold Spring Harb. Perspect. Med.* **2012,** *2*, a006213.

20. Hort, J.; O’brien, J.; Gainotti, G.; Pirttila, T.; Popescu, B.; Rektorova, I.; Sorbi, S.; Scheltens, P.; Dementia, E. S. P. o. EFNS guidelines for the diagnosis and management of Alzheimer’s disease. *Eur. J. Neurol.* **2010,** *17*, 1236-1248.

21. Frisoni, G. B.; Fox, N. C.; Jack, C. R.; Scheltens, P.; Thompson, P. M. The clinical use of structural MRI in Alzheimer disease. *Nat. Rev. Neurol.* **2010,** *6*, 67-77.

22. Barthel, H.; Schroeter, M. L.; Hoffmann, K.-T.; Sabri, O. PET/MR in Dementia and Other Neurodegenerative Diseases. *Semin. Nucl. Med.* **2015,** *45*, 224-233.

23. Mattsson, N.; Blennow, K.; Zetterberg, H. CSF biomarkers. *Ann. N.Y. Acad. Sci.* **2009,** *1180*, 28-35.

24. DeMarshall, C. A.; Nagele, E. P.; Sarkar, A.; Acharya, N. K.; Godsey, G.; Goldwaser, E. L.; Kosciuk, M.; Thayasivam, U.; Han, M.; Belinka, B.; Nagele, R. G. Detection of Alzheimer's disease at mild cognitive impairment and disease progression using autoantibodies as blood-based biomarkers. *Alzheimer's & Dementia: Diagnosis, Assessment & Disease Monitoring* **2016,** *3*, 51-62.

25. Chen, Z.; Zhong, C. Decoding Alzheimer's disease from perturbed cerebral glucose metabolism: Implications for diagnostic and therapeutic strategies. *Prog. Neurobiol.* **2013,** *108*, 21-43.

26. Drzezga, A.; Barthel, H.; Minoshima, S.; Sabri, O. Potential clinical applications of PET/MR imaging in neurodegenerative diseases. *J. Nucl. Med.* **2014**, jnumed. 113.129254.

27. Nagele, E. P.; Han, M.; Acharya, N. K.; DeMarshall, C.; Kosciuk, M. C.; Nagele, R. G. Natural IgG autoantibodies are abundant and ubiquitous in human sera, and their number is influenced by age, gender, and disease. *PLoS One* **2013,** *8*, e60726.

28. Reddy, M. M.; Wilson, R.; Wilson, J.; Connell, S.; Gocke, A.; Hynan, L.; German, D.; Kodadek, T. Identification of Candidate IgG Biomarkers for Alzheimer's Disease via Combinatorial Library Screening. *Cell* **2011,** *144*, 132-142.

29. Nagele, E.; Han, M.; DeMarshall, C.; Belinka, B.; Nagele, R. Diagnosis of Alzheimer's disease based on disease-specific autoantibody profiles in human sera. *PLoS One* **2011,** *6*, e23112.

30. Peskind, E. R.; Riekse, R.; Quinn, J. F.; Kaye, J.; Clark, C. M.; Farlow, M. R.; Decarli, C.; Chabal, C.; Vavrek, D.; Raskind, M. A. Safety and acceptability of the research lumbar puncture. *Alzheimer Dis. Assoc. Disord.* **2005,** *19*, 220-225.

31. Clark, C. M.; Schneider, J. A.; Bedell, B. J.; et al. Use of florbetapir-pet for imaging β-amyloid pathology. *JAMA* **2011,** *305*, 275-283.

32. Sehlin, D.; Fang, X. T.; Cato, L.; Antoni, G.; Lannfelt, L.; Syvänen, S. Antibody-based PET imaging of amyloid beta in mouse models of Alzheimer's disease. *Nat. Commun.* **2016,** *7*, 10759.

33. Matharu, B.; Spencer, N.; Howe, F.; Austen, B. Gadolinium-complexed Aβ-binding contrast agents for MRI diagnosis of Alzheimer's Disease. *Neuropeptides* **2015,** *53*, 63-70.

34. Santin, M. D.; Debeir, T.; Bridal, S. L.; Rooney, T.; Dhenain, M. Fast in vivo imaging of amyloid plaques using μ-MRI Gd-staining combined with ultrasound-induced blood–brain barrier opening. *NeuroImage* **2013,** *79*, 288-294.

35. Sigurdsson, E. M.; Wadghiri, Y. Z.; Mosconi, L.; Blind, J. A.; Knudsen, E.; Asuni, A.; Scholtzova, H.; Tsui, W. H.; Li, Y.; Sadowski, M.; Turnbull, D. H.; de Leon, M. J.; Wisniewski, T. A non-toxic ligand for voxel-based MRI analysis of plaques in AD transgenic mice. *Neurobiol. Aging* **2008,** *29*, 836-847.

36. Hamers-Casterman, C.; Atarhouch, T.; Muyldermans, S.; Robinson, G.; Hammers, C.; Songa, E. B.; Bendahman, N.; Hammers, R. Naturally occurring antibodies devoid of light chains. *Nature* **1993,** *363*, 446.

37. Li, T.; Bourgeois, J.-P.; Celli, S.; Le Sourd, A.-M.; Mecheri, S.; Weksler, B.; Romero, I.; Couraud, P.-O.; Rougeon, F.; Lafaye, P. Cell-penetrating anti-GFAP VHH and corresponding fluorescent fusion protein VHH-GFP spontaneously cross the blood-brain barrier and specifically recognize astrocytes: application to brain imaging. *FASEB J.* **2012,** *26*, 3969-3979.

38. Nabuurs, R. J. A.; Rutgers, K. S.; Welling, M. M.; Metaxas, A.; de Backer, M. E.; Rotman, M.; Bacskai, B. J.; van Buchem, M. A.; van der Maarel, S. M.; van der Weerd, L. In Vivo Detection of Amyloid-β Deposits Using Heavy Chain Antibody Fragments in a Transgenic Mouse Model for Alzheimer's Disease. *PLoS One* **2012,** *7*, e38284.

39. Rotman, M.; Welling, M. M.; Bunschoten, A.; de Backer, M. E.; Rip, J.; Nabuurs, R. J. A.; Gaillard, P. J.; van Buchem, M. A.; van der Maarel, S. M.; van der Weerd, L. Enhanced glutathione PEGylated liposomal brain delivery of an anti-amyloid single domain antibody fragment in a mouse model for Alzheimer's disease. *J. Control. Release* **2015,** *203*, 40-50.

40. Li, T.; Vandesquille, M.; Koukouli, F.; Dudeffant, C.; Youssef, I.; Lenormand, P.; Ganneau, C.; Maskos, U.; Czech, C.; Grueninger, F.; Duyckaerts, C.; Dhenain, M.; Bay, S.; Delatour, B.; Lafaye, P. Camelid single-domain antibodies: A versatile tool for in vivo imaging of extracellular and intracellular brain targets. *J. Control. Release* **2016,** *243*, 1-10.

41. Cummings, J. L.; Morstorf, T.; Zhong, K. Alzheimer's disease drug-development pipeline: few candidates, frequent failures. *Alzheimer's Res. Ther.* **2014,** *6*, 37.

42. Wollen, K. A. Alzheimer's disease: the pros and cons of pharmaceutical, nutritional, botanical, and stimulatory therapies, with a discussion of treatment strategies from the perspective of patients and practitioners. *Altern. Med. Rev.* **2010,** *15*, 223-44.

43. Eleti, S. Drugs in Alzheimer's disease Dementia: An overview of current pharmacological management and future directions. *Psychiatr. Danub.* **2016,** *28*, 136-140.

44. Wang, R.; Reddy, P. H. Role of glutamate and NMDA receptors in Alzheimer's disease. *J. Alzheimer's Dis.* **2017,** *57*, 1041-1048.

45. Giacobini, E. Cholinesterases: New Roles in Brain Function and in Alzheimer's Disease. *Neurochem. Res.* **2003,** *28*, 515-522.

46. Rygiel, K. Novel strategies for Alzheimer's disease treatment: An overview of anti-amyloid beta monoclonal antibodies. *Indian J. Pharmacol.* **2016,** *48*, 629-636.

47. Panza, F.; Solfrizzi, V.; Frisardi, V.; Capurso, C.; D'Introno, A.; Colacicco, A. M.; Vendemiale, G.; Capurso, A.; Imbimbo, B. P. Disease-Modifying Approach to the Treatment of Alzheimer's Disease. *Drugs Aging* **2009,** *26*, 537-555.

48. Kumar, D.; Ganeshpurkar, A.; Kumar, D.; Modi, G.; Gupta, S. K.; Singh, S. K. Secretase inhibitors for the treatment of Alzheimer's disease: Long road ahead. *Eur. J. Med. Chem.* **2018,** *148*, 436-452.

49. Wisniewski, T.; Goñi, F. Immunotherapeutic Approaches for Alzheimer's Disease. *Neuron* **2015,** *85*, 1162-1176.

50. van Dyck, C. H. Anti-Amyloid-β Monoclonal Antibodies for Alzheimer's Disease: Pitfalls and Promise. *Biol. Psychiatry* **2018,** *83*, 311-319.

51. Sterner, R. M.; Takahashi, P. Y.; Yu Ballard, A. C. Active Vaccines for Alzheimer Disease Treatment. *J. Am. Med. Dir. Assoc.* **2016,** *17*, 862.e11-862.e15.

52. Grauer, A.; König, B. Peptidomimetics – A Versatile Route to Biologically Active Compounds. *Eur. J. Org. Chem.* **2009,** *2009*, 5099-5111.

53. Zorzi, A.; Deyle, K.; Heinis, C. Cyclic peptide therapeutics: past, present and future. *Curr. Opin. Chem. Biol.* **2017,** *38*, 24-29.

54. Abdalla, M.; McGaw, L. Natural Cyclic Peptides as an Attractive Modality for Therapeutics: A Mini Review. *Molecules* **2018,** *23*, 2080.

55. Joo, S. H. Cyclic peptides as therapeutic agents and biochemical tools. *Biomolecules & therapeutics* **2012,** *20*, 19-26.

56. Ghadiri, M. R.; Granja, J. R.; Milligan, R. A.; McRee, D. E.; Khazanovich, N. Self-assembling organic nanotubes based on a cyclic peptide architecture. *Nature* **1993,** *366*, 324.

57. Fernandez-Lopez, S.; Kim, H.-S.; Choi, E. C.; Delgado, M.; Granja, J. R.; Khasanov, A.; Kraehenbuehl, K.; Long, G.; Weinberger, D. A.; Wilcoxen, K. M. Antibacterial agents based on the cyclic D, L-α-peptide architecture. *Nature* **2001,** *412*, 452.

58. Davies, J. S. The cyclization of peptides and depsipeptides. *J. Pept. Sci.* **2003,** *9*, 471-501.

59. Lawson, K. V.; Rose, T. E.; Harran, P. G. Template-constrained macrocyclic peptides prepared from native, unprotected precursors. *Proc. Natl. Acad. Sci.* **2013,** *110*, E3753-E3760.

60. Wu, J.; Tang, J.; Chen, H.; He, Y.; Wang, H.; Yao, H. Recent Developments in Peptide Macrocyclization. *Tetrahedron Lett.* **2017**.

61. White, C. J.; Yudin, A. K. Contemporary strategies for peptide macrocyclization. *Nature chemistry* **2011,** *3*, 509.

62. Martí-Centelles, V.; Pandey, M. D.; Burguete, M. I.; Luis, S. V. Macrocyclization Reactions: The Importance of Conformational, Configurational, and Template-Induced Preorganization. *Chem. Rev.* **2015,** *115*, 8736-8834.

63. Malesevic, M.; Strijowski, U.; Bächle, D.; Sewald, N. An improved method for the solution cyclization of peptides under pseudo-high dilution conditions. *J. Biotechnol.* **2004,** *112*, 73-77.

64. Tapeinou, A.; Matsoukas, M. T.; Simal, C.; Tselios, T. Review cyclic peptides on a merry-go-round; towards drug design. *Pept. Sci.* **2015,** *104*, 453-461.

65. Collins, J. M.; Porter, K. A.; Singh, S. K.; Vanier, G. S. High-Efficiency Solid Phase Peptide Synthesis (HE-SPPS). *Org. Lett.* **2014,** *16*, 940-943.

66. Kumar, A.; Jad, Y. E.; Collins, J. M.; Albericio, F.; de la Torre, B. G. Microwave-Assisted Green Solid-Phase Peptide Synthesis Using γ-Valerolactone (GVL) as Solvent. *ACS Sustainable Chemistry & Engineering* **2018,** *6*, 8034-8039.

67. Lambert, J. N.; Mitchell, J. P.; Roberts, K. D. The synthesis of cyclic peptides. *J. Chem. Soc., Perkin Trans. 1* **2001**, 471-484.

68. Romanovskis, P.; Spatola, A. Preparation of head-to-tail cyclic peptides via side-chain attachment: Implications for library synthesis. *J. Pept. Res.* **1998,** *52*, 356-374.

69. Kates, S. A.; Solé, N. A.; Johnson, C. R.; Hudson, D.; Barany, G.; Albericio, F. A novel, convenient, three-dimensional orthogonal strategy for solid-phase synthesis of cyclic peptides. *Tetrahedron Lett.* **1993,** *34*, 1549-1552.

70. Cudic, M.; Wade, J. D.; Otvos, J. L. Convenient synthesis of a head-to-tail cyclic peptide containing an expanded ring. *Tetrahedron Lett.* **2000,** *41*, 4527-4531.

71. Ghadiri, M. R.; Granja, J. R.; Buehler, L. K. Artificial transmembrane ion channels from self-assembling peptide nanotubes. *Nature* **1994,** *369*, 301.

72. Granja, J. R.; Ghadiri, M. R. Channel-mediated transport of glucose across lipid bilayers. *J. Am. Chem. Soc.* **1994,** *116*, 10785-10786.

73. Sánchez-Quesada, J.; Isler, M. P.; Ghadiri, M. R. Modulating ion channel properties of transmembrane peptide nanotubes through heteromeric supramolecular assemblies. *J. Am. Chem. Soc.* **2002,** *124*, 10004-10005.

74. Vollmer, M. S.; Clark, T. D.; Steinem, C.; Ghadiri, M. R. Photoswitchable hydrogen-bonding in self-organized cylindrical peptide systems. *Angew. Chem. Int. Ed.* **1999,** *38*, 1598-1601.

75. Steinem, C.; Janshoff, A.; Vollmer, M. S.; Ghadiri, M. R. Reversible Photoisomerization of Self-Organized Cylindrical Peptide Assemblies at Air− Water and Solid Interfaces. *Langmuir* **1999,** *15*, 3956-3964.

76. Motesharei, K.; Ghadiri, M. R. Diffusion-limited size-selective ion sensing based on SAM-supported peptide nanotubes. *J. Am. Chem. Soc.* **1997,** *119*, 11306-11312.

77. Motiei, L.; Rahimipour, S.; Thayer, D. A.; Wong, C.-H.; Ghadiri, M. R. Antibacterial cyclic d, l-α-glycopeptides. *ChemComm* **2009**, 3693-3695.

78. Montero, A.; Gastaminza, P.; Law, M.; Cheng, G.; Chisari, F. V.; Ghadiri, M. R. Self-assembling peptide nanotubes with antiviral activity against hepatitis C virus. *Chem. Biol.* **2011,** *18*, 1453-1462.

79. Horne, W. S.; Ashkenasy, N.; Ghadiri, M. R. Modulating charge transfer through cyclic d, l-α-peptide self-assembly. *Chem. Eur. J.* **2005,** *11*, 1137-1144.

80. Ashkenasy, N.; Horne, W. S.; Ghadiri, M. R. Design of self-assembling peptide nanotubes with delocalized electronic states. *Small* **2006,** *2*, 99-102.

81. Shapira, R.; Rudnick, S.; Daniel, B.; Viskind, O.; Aisha, V.; Richman, M.; Ayasolla, K. R.; Perelman, A.; Chill, J. H.; Gruzman, A. Multifunctional cyclic D, L-α-peptide architectures stimulate non-insulin dependent glucose uptake in skeletal muscle cells and protect them against oxidative stress. *J. Med. Chem.* **2013,** *56*, 6709-6718.

82. Bong, D. T.; Clark, T. D.; Granja, J. R.; Ghadiri, M. R. Self-assembling organic nanotubes. *Angew. Chem. Int. Ed.* **2001,** *40*, 988-1011.

83. De Santis, P.; Morosetti, S.; Rizzo, R. Conformational analysis of regular enantiomeric sequences. *Macromolecules* **1974,** *7*, 52-58.

84. Ramachnandran, G.; Chandrasekaran, R. Conformation of peptide chains containing both L- & D-residues. I. Helical structures with alternating L-& D-residues with special reference to the LD-ribbon & the LD-helices. *Indian J. Biochem. Biophys.* **1972,** *9*, 1.

85. Bong, D.; Clark, T.; Granja, J.; Ghadiri, M. Tubular organic materials. *Angew. Chem., Int. Ed* **2001,** *40*, 988-1011.

86. Lührs, T.; Ritter, C.; Adrian, M.; Riek-Loher, D.; Bohrmann, B.; Döbeli, H.; Schubert, D.; Riek, R. 3D structure of Alzheimer's amyloid-β (1–42) fibrils. *Proc. Natl. Acad. Sci.* **2005,** *102*, 17342-17347.

87. Richman, M.; Wilk, S.; Chemerovski, M.; Wärmländer, S. K.; Wahlström, A.; Gräslund, A.; Rahimipour, S. In vitro and mechanistic studies of an antiamyloidogenic self-assembled cyclic d, l-α-peptide architecture. *J. Am. Chem. Soc.* **2013,** *135*, 3474-3484.

88. Chemerovski-Glikman, M.; Richman, M.; Rahimipour, S. Structure-based study of antiamyloidogenic cyclic d, l-α-peptides. *Tetrahedron* **2014,** *70*, 7639-7644.

89. Proulx, C.; Sabatino, D.; Hopewell, R.; Spiegel, J.; García Ramos, Y.; Lubell, W. D. Azapeptides and their therapeutic potential. *Future Med. Chem.* **2011,** *3*, 1139-1164.

90. Gante, J. Azapeptides, A Novel Class of Peptide Analogs. *Angew. Chem., Int. Ed* **1970,** *9*, 813-813.

91. Gante, J. Azapeptides. *Synthesis* **1989,** *21*, 405-413.

92. Zega, A.; Urleb, U. Azapeptides. *Acta Chim. Slov.* **2002,** *49*, 649-662.

93. Zega, A. Azapeptides as pharmacological agents. *Curr. Med. Chem.* **2005,** *12*, 589-597.

94. Thormann, M.; Hofmann, H.-J. Conformational properties of azapeptides. *J. Mol. Struct. THEOCHEM* **1999,** *469*, 63-76.

95. Boeglin, D.; Lubell, W. D. Aza-amino acid scanning of secondary structure suited for solid-phase peptide synthesis with Fmoc chemistry and aza-amino acids with heteroatomic side chains. *J. Comb. Chem.* **2005,** *7*, 864-878.

96. Melendez, R. E.; Lubell, W. D. Aza-amino acid scan for rapid identification of secondary structure based on the application of N-Boc-Aza1-dipeptides in peptide synthesis. *J. Am. Chem. Soc.* **2004,** *126*, 6759-6764.

97. Lee, H.-J.; Song, J.-W.; Choi, Y.-S.; Park, H.-M.; Lee, K.-B. A theoretical study of conformational properties of N-methyl azapeptide derivatives. *J. Am. Chem. Soc.* **2002,** *124*, 11881-11893.

98. Lee, H.-J.; Jung, H. J.; Kim, J. H.; Park, H.-M.; Lee, K.-B. Conformational preference of azaglycine-containing dipeptides studied by PCM and IPCM methods. *Chem. Phys.* **2003,** *294*, 201-210.

99. Lee, H. J.; Lee, K. B.; Ahn, I. A.; Ro, S.; Choi, K. H.; Choi, Y. S. Role of azaamino acid residue in β-turn formation and stability in designed peptide. *J. Pept. Res.* **2000,** *56*, 35-46.

100. Hess, H.-J.; Moreland, W. T.; Laubach, G. D. N-[2-Isopropyl-3-(L-aspartyl-L-arginyl)-carbazoyl]-L-tyrosyl-L-valyl-L-histidyl-L-prolyl-L-phenylalanine, 1 an Isostere of Bovine Angiotensin II. *J. Am. Chem. Soc.* **1963,** *85*, 4040-4041.

101. Bailey, M. D.; Halmos, T.; Goudreau, N.; Lescop, E.; Llinàs-Brunet, M. Novel Azapeptide Inhibitors of Hepatitis C Virus Serine Protease. *J. Med. Chem.* **2004,** *47*, 3788-3799.

102. Graybill, T. L.; Ross, M. J.; Gauvin, B. R.; Gregory, J. S.; Harris, A. L.; Ator, M. A.; Rinker, J. M.; Dolle, R. E. Synthesis and evaluation of azapeptide-derived inhibitors of serine and cysteine proteases. *Bioorg. Med. Chem. Lett.* **1992,** *2*, 1375-1380.

103. Sverrisdottir, A.; Nystedt, M.; Johansson, H.; Fornander, T. Adjuvant goserelin and ovarian preservation in chemotherapy treated patients with early breast cancer: results from a randomized trial. *Breast Cancer Res. Treat.* **2009,** *117*, 561.

104. Dutta, A. S.; Furr, B. J.; Giles, M. B.; Valcaccia, B. Synthesis and biological activity of highly active. alpha.-aza analogs of luliberin. *J. Med. Chem.* **1978,** *21*, 1018-1024.

105. Dutta, A. S.; Furr, B. J.; Giles, M. B. Polypeptides. Part 15. Synthesis and biological activity of α-aza-analogues of luliberin modified in positions 6 and 10. *J. Chem. Soc., Perkin Trans. 1* **1979**, 379-388.

106. von Hentig, N. Atazanavir/ritonavir: a review of its use in HIV therapy. *Drugs Today* **2008,** *44*, 103.

107. Piliero, P. J. Atazanavir: a novel HIV-1 protease inhibitor. *Expert Opin. Investig. Drugs* **2002,** *11*, 1295-1301.

108. Gianotti, N.; Lazzarin, A. Atazanavir/ritonavir: a valuable once-daily HIV protease inhibitor with little impact on lipid profile. *Future Virol.* **2007,** *2*, 131-143.

109. Gray, C. J.; Ireson, J. C.; Parker, R. C. Preparation and properties of some α-aza-amino-acid derivatives, their possible use in peptide synthesis. *Tetrahedron* **1977,** *33*, 739-743.

110. Quibell, M.; Turnell, W. G.; Johnson, T. Synthesis of azapeptides by the Fmoc/tert-butyl/polyamide technique. *J. Chem. Soc., Perkin Trans. 1* **1993**, 2843-2849.

111. Gray, C.; Quibell, M.; Jiang, K.-L.; Baggett, N. Synthesis and spectroscopic properties of azaglutamine amino acid and peptide derivatives. *Synthesis* **1991,** *1991*, 141-146.

112. Liley, M.; Johnson, T. Solid phase synthesis of azapeptides utilising reversible amide bond protection to prevent hydantoin formation. *Tetrahedron Lett.* **2000,** *41*, 3983-3985.

113. Frochot, C.; Vanderesse, R.; Driou, A.; Linden, G.; Marraud, M.; Thong Cung, M. A solid-phase synthesis of three aza-, iminoaza- and reduced aza-peptides from the same precursor. *Lett. Pept. Sci.* **1997,** *4*, 219-225.

114. Zega, A.; Mlinšek, G.; Šepic, P.; Golič Grdadolnik, S.; Šolmajer, T.; Tschopp, T. B.; Steiner, B.; Kikelj, D.; Urleb, U. Design and structure–activity relationship of thrombin inhibitors with an azaphenylalanine scaffold: potency and selectivity enhancements via P2 optimization. *Biorg. Med. Chem.* **2001,** *9*, 2745-2756.

115. Gibson, C.; Goodman, S. L.; Hahn, D.; Hölzemann, G.; Kessler, H. Novel solid-phase synthesis of azapeptides and azapeptoides via Fmoc-strategy and its application in the synthesis of RGD-mimetics. *J. Org. Chem.* **1999,** *64*, 7388-7394.

116. Sulyok, G. A.; Gibson, C.; Goodman, S. L.; Hölzemann, G.; Wiesner, M.; Kessler, H. Solid-phase synthesis of a nonpeptide RGD mimetic library: new selective αvβ3 integrin antagonists. *J. Med. Chem.* **2001,** *44*, 1938-1950.

117. Murphy, A. M.; Dagnino Jr, R.; Vallar, P. L.; Trippe, A. J.; Sherman, S. L.; Lumpkin, R. H.; Tamura, S. Y.; Webb, T. R. Automated synthesis of peptide C-terminal aldehydes. *J. Am. Chem. Soc.* **1992,** *114*, 3156-3157.

118. Wieczerzak, E.; Drabik, P.; Łankiewicz, L.; Ołdziej, S.; Grzonka, Z.; Abrahamson, M.; Grubb, A.; Brömme, D. Azapeptides Structurally Based upon Inhibitory Sites of Cystatins as Potent and Selective Inhibitors of Cysteine Proteases. *J. Med. Chem.* **2002,** *45*, 4202-4211.

119. Mhidia, R.; Melnyk, O. Selective cleavage of an azaGly peptide bond by copper(II). Long-range effect of histidine residue. *J. Pept. Sci.* **2010,** *16*, 141-147.

120. Garcia-Ramos, Y.; Lubell, W. D. Synthesis and alkylation of aza-glycinyl dipeptide building blocks. *J. Pept. Sci.* **2013,** *19*, 725-729.

121. Chingle, R.; Proulx, C.; Lubell, W. D. Azapeptide synthesis methods for expanding side-chain diversity for biomedical applications. *Acc. Chem. Res.* **2017,** *50*, 1541-1556.

122. Bourguet, C. B.; Sabatino, D.; Lubell, W. D. Benzophenone semicarbazone protection strategy for synthesis of aza-glycine containing aza-peptides. *Pept. Sci.* **2008,** *90*, 824-831.

123. Bourguet, C. B.; Proulx, C.; Klocek, S.; Sabatino, D.; Lubell, W. D. Solution-phase submonomer diversification of aza-dipeptide building blocks and their application in aza-peptide and aza-DKP synthesis. *J. Pept. Sci.* **2010,** *16*, 284-296.

124. Reynolds, C. H.; Hormann, R. E. Theoretical study of the structure and rotational flexibility of diacylhydrazines: Implications for the structure of nonsteroidal ecdysone agonists and azapeptides. *J. Am. Chem. Soc.* **1996,** *118*, 9395-9401.

125. Niedrich, H.; Oehme, C. Hydrazinverbindungen als Heterobestandteile in Peptiden. XV. Synthese von Eledoisin-Octapeptiden mit den Carbazylresten Azaglycin und α-Azaasparagin statt Glycin und Asparagin. *J. prakt. Chem.* **1972,** *314*, 759-768.

126. Goodman, S. L.; Hölzemann, G.; Sulyok, G. A.; Kessler, H. Nanomolar small molecule inhibitors for αvβ6, αvβ5, and αvβ3 integrins. *J. Med. Chem.* **2002,** *45*, 1045-1051.

127. Gibson, C.; Sulyok, G. A.; Hahn, D.; Goodman, S. L.; Hölzemann, G.; Kessler, H. Nonpeptidic αvβ3 Integrin Antagonist Libraries: On-Bead Screening and Mass Spectrometric Identification without Tagging. *Angew. Chem. Int. Ed.* **2001,** *40*, 165-169.

128. Spiegel, J.; Mas-Moruno, C.; Kessler, H.; Lubell, W. D. Cyclic aza-peptide integrin ligand synthesis and biological activity. *J. Org. Chem.* **2012,** *77*, 5271-5278.

129. Boeglin, D.; Hamdan, F. F.; Melendez, R. E.; Cluzeau, J.; Laperriere, A.; Héroux, M.; Bouvier, M.; Lubell, W. D. Calcitonin Gene-Related Peptide Analogues with Aza and Indolizidinone Amino Acid Residues Reveal Conformational Requirements for Antagonist

Activity at the Human Calcitonin Gene-Related Peptide 1 Receptor. *J. Med. Chem.* **2007,** *50*, 1401-1408.

130. Zhang, Y.; Malamakal, R. M.; Chenoweth, D. M. Aza-glycine induces collagen hyperstability. *J. Am. Chem. Soc.* **2015,** *137*, 12422-12425.

131. Kasznel, A. J.; Zhang, Y.; Hai, Y.; Chenoweth, D. M. Structural Basis for Aza-Glycine Stabilization of Collagen. *J. Am. Chem. Soc.* **2017,** *139*, 9427-9430.

Chapter 2: Azacyclopeptide synthesis and neuroprotective activity against Aβ toxicity

2.1. Hypothesis:

Introduction of aza-residues into the backbone of cyclic D,L-α-peptides was explored to study their impact on aggregation and anti-amyloidogenic activity (Figure 2.1). Azapeptides may improve hydrogen bonding. Replacement of the Cα carbon with a more electronegative Nα may increase the acidity of the amide NH adjacent to the α-nitrogen. Introduction of aza-glycine may add an additional hydrogen bond donor to strengthen intermolecular hydrogen bonding.

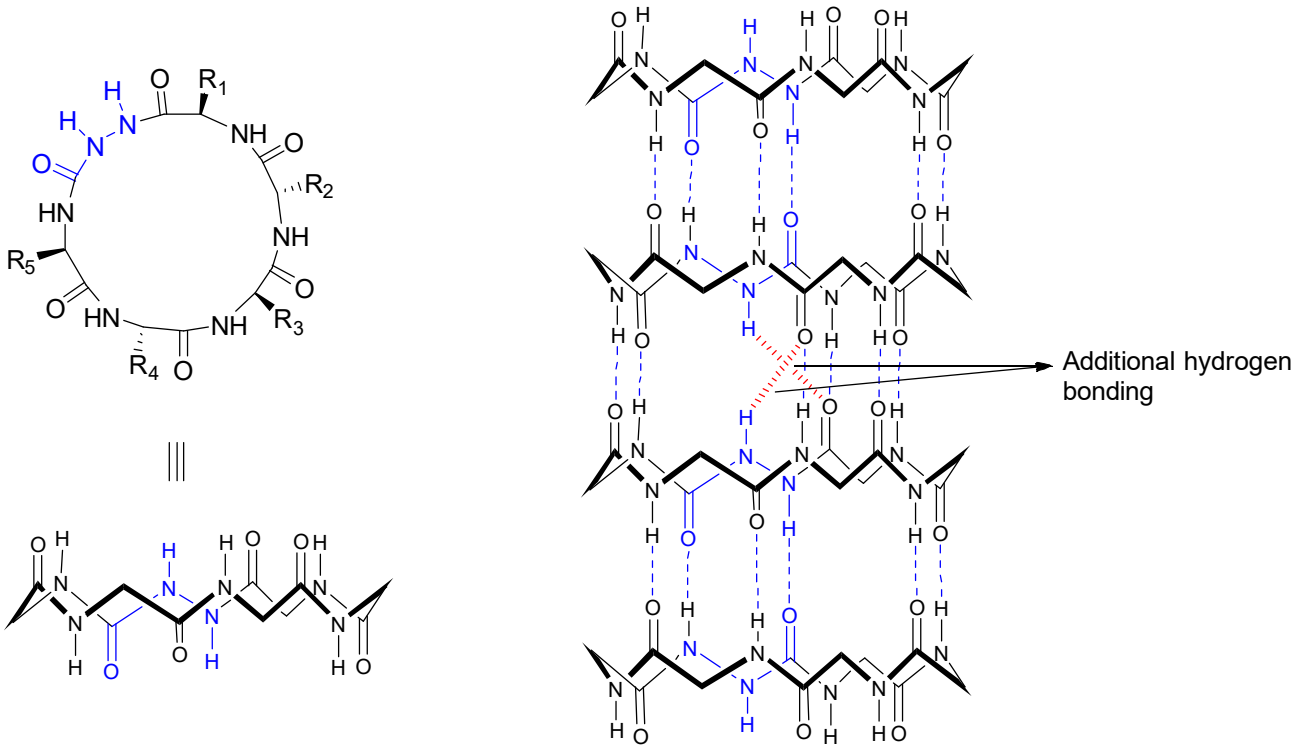

Figure 2.1: Cyclic D,L-α-azapeptide self-assembly may be stabilized through improved hydrogen bonding interactions of aza-glycine residues (Hypothetical)

2.2. Results and Discussion

An aza-amino acid scan of the sequence of **CP-2** has been pursued to examine the impact on the aggregation and biological activity of the cyclic D,L-α-peptide upon replacement of each

amino amide with a semicarbazide. Insertion of a semicarbazide was expected to improve the potential for self-assembly by increasing hydrogen bonding propensity of the cycle.[1-2] In particular, each amino acid in the sequence of **CP-2** was systematically replaced by aza-glycine to add a second hydrogen donor at the expense of losing the amino acid side chain. All six [azaG]-**CP-2** analogues were prepared. (Figure 2.2).

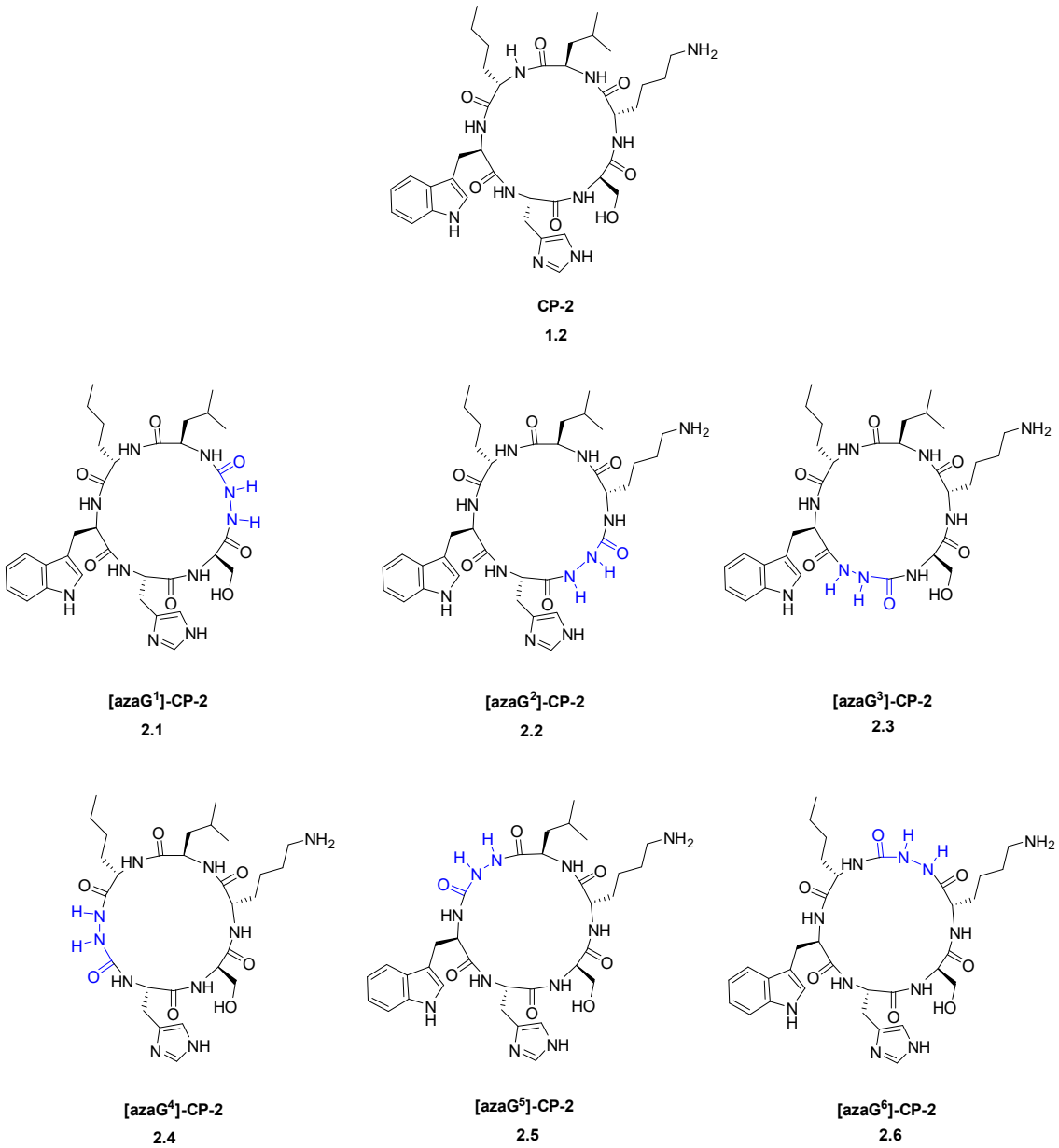

Figure 2.2: Aza-glycine **CP-2** analogues

Three different approaches were employed to synthesize the six [azaG]-**CP-2** analogues. Elongation and cyclization were performed on solid-phase in most cases. In two cases, macrocycle formation was performed in solution. Three azapeptides (e.g., **2.3-2.5**) were synthesized using Method I, which entailed linking the lysine side chain to the solid support, peptide elongation with aza-glycine incorporation, and head-to-tail macrocyclization, prior to resin cleavage and purification. Azapeptide **2.2** was prepared by employing Method II, which involved a modification of the latter strategy in which protection of the α-nitrogen of the aza-glycine residue was required to avoid side product formation. The two remaining azapeptides (e.g., **2.1** and **2.6**) were synthesized using Method III, which employed sequence elongation on solid phase, resin cleavage without side chain removal, head-to-tail macrocyclization in solution, followed by unmasking of the side chains and purification.

Scheme 2.1: General strategy for the synthesis of azapeptides **2.3-2.5** (Method-I)

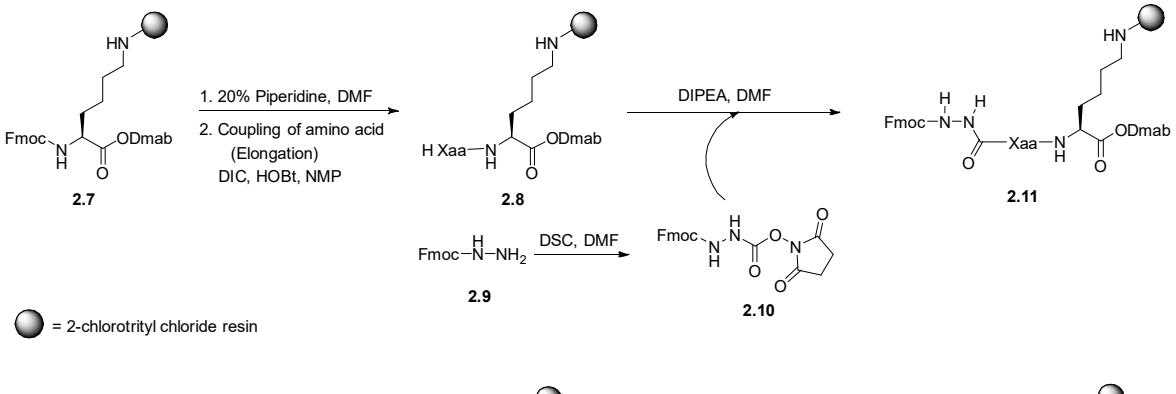

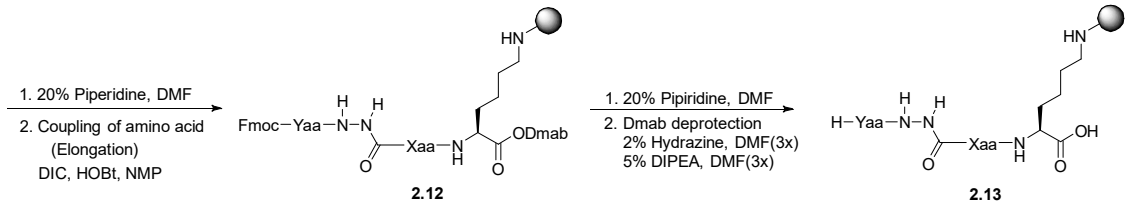

1. Head to tail cyclization
DIC, HOBt, NMP
2. Resin clevage
TFA, TES, H_2O
(95 : 2.5 : 2.5)

Azacyclic peptide
(2.3-2.5)

Xaa	Yaa	Cyclicpeptide
D-Ser(tBu)	D-Leu-Nle-D-Trp(Boc)	**[azaG^3]-CP-2** (2.3)
His-D-Ser(tBu)	D-Leu-Nle	**[azaG^4]-CP-2** (2.4)
D-Trp(Boc)-His(Trt)-D-Ser(tBu)	D-Leu	**[azaG^5]-CP-2** (2.5)

Cyclic azapeptides **2.3-2.5** were pursued using a common solid-phase protocol (Method I, Scheme 2.1). The solid supported Fmoc-Lys-ODmab **2.7** was synthesized starting from N^{α}-(Fmoc)-N^{ε}-(Boc)lysine **2.14**, which was converted to the 4-{*N*-[1-(4,4-dimethyl-2,6-dioxocyclohexylidene)-3-methylbutyl]amino}benzyl (Dmab) ester **2.16** according to the published procedure,[3-4] and treated with 50% TFA in DCM to afford Fmoc-Lys-ODmab (**2.17**). The ε-amine **2.17** was reacted with 2-chlorotrityl chloride polystyrene resin using DIPEA in DCM to provide lysine resin **2.7** (Scheme 2.2).

Scheme 2.2: General strategy for the synthesis of solid supported lysine **2.7**

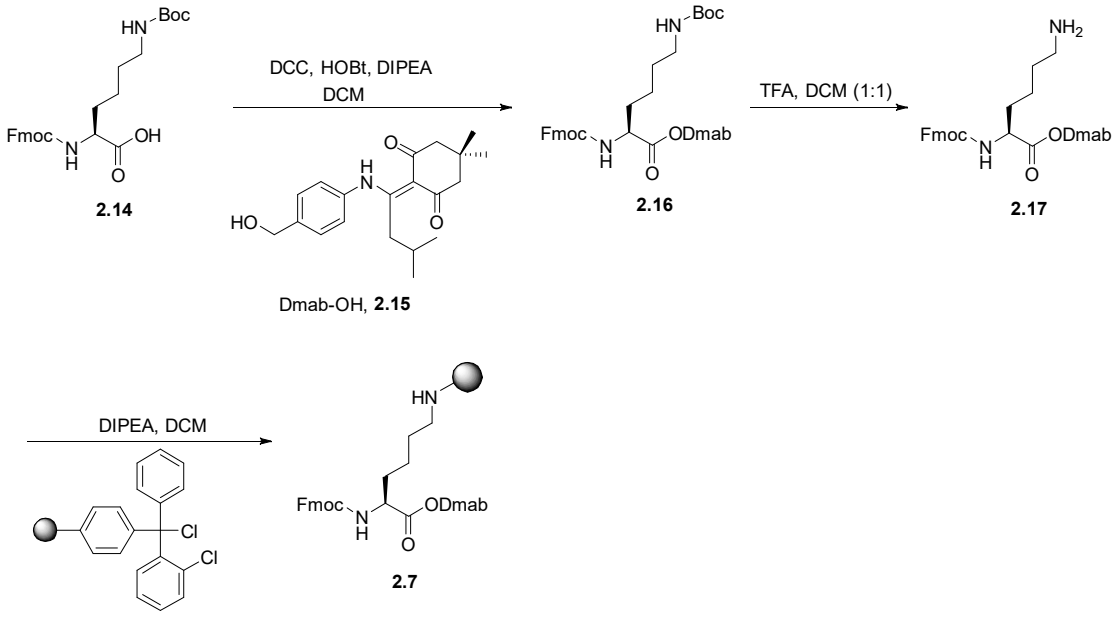

The Dmab carboxylate protection offered stability towards piperidine in DMF, conditions used to remove the Fmoc group, and provided capacity for removal without resin cleavage. The Dmab group was removed from the carboxylate by a two-step process featuring severing of the 1-(4,4-dimethyl-2,6-dioxocyclohexylidene)-3-methylbutyl (Dde) moiety on treatment with 2% hydrazine in DMF to form indazole by-product **2.19**, followed by 1,6-elimination of the resulting *p*-amino benzyl ester **2.20** on treatment with 5% DIPEA in DMF (Scheme 2.3).[5-6] Although 1,6-

elimination may be a spontaneous process, DIPEA was used to accelerate *p*-amino benzyl ester removal, the rate of which may be peptide sequence dependant.

Scheme 2.3: Dmab protection group removal

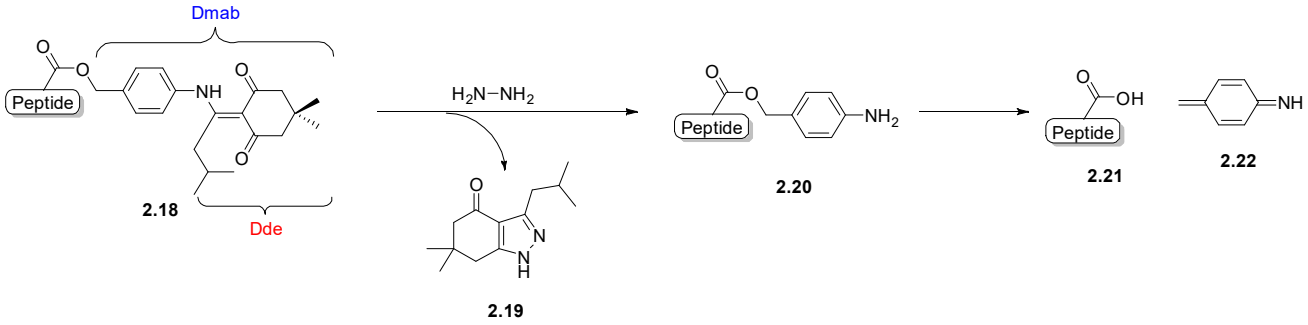

The aza-Gly residue was added to the peptide sequence using active carbazate **2.10**, which was formed on treatment of *N*-(Fmoc)hydrazine (**2.9**) with *N,N'*-disuccinimidyl carbonate (DSC).[7-8] Employing DSC in the aza-glycine coupling protocol avoided intramolecular cyclization after activation of the aza-residue to form oxadiazolone, which has been observed using more reactive reagents such as carbonyldiimidazole (CDI) and phosgene.[9-10]

Starting from Fmoc-Lys-ODmab resin **2.7**, the linear peptide sequence of [azaG^5]-**CP-2** (**2.5**) was elongated using standard solid-phase synthesis methods. Piperidine in DMF was used to remove the Fmoc group. The amino acid residues Fmoc-D-Ser(tBu)-OH, Fmoc-His(Tr)-OH and Fmoc-D-Trp(Boc)-OH were coupled to the growing peptide chain using DIC and HOBt in NMP.[11] After introduction of Fmoc-aza-Gly-OSu and Fmoc removal, Fmoc-D-Leu-OH was added to the sequence. The Fmoc and Dmab protecting groups were removed and cyclization was performed using DIC and HOBt in NMP.[12] Resin cleavage, azapeptide precipitation and subsequent purification by reverse-phase HPLC provided [azaG^5]-**CP-2** (**2.5**).

Both [azaG^3]-**CP-2** and [azaG^4]-**CP-2** (**2.3** and **2.4**) were synthesized using similar chemistry as described for [azaG^5]-**CP-2** (**2.5**) starting from Fmoc-Lys-ODmab resin **2.7** with peptide elongations, aza-residue incorporation, and further elongations using Fmoc-D-Ser(tBu)-OH, Fmoc-His(Trt)-OH, (Fmoc-D-Trp(Boc)-OH, Fmoc-Nle-OH and Fmoc-D-Leu-OH, respectively. Removal of the *N*- and *C*-terminal residue protection, cyclization, resin cleavage and purification were performed as described above to provide azapeptides **2.3** and **2.4**.

Scheme 2.4: Cyclization of aza-glycinyl tripeptide **2.23**

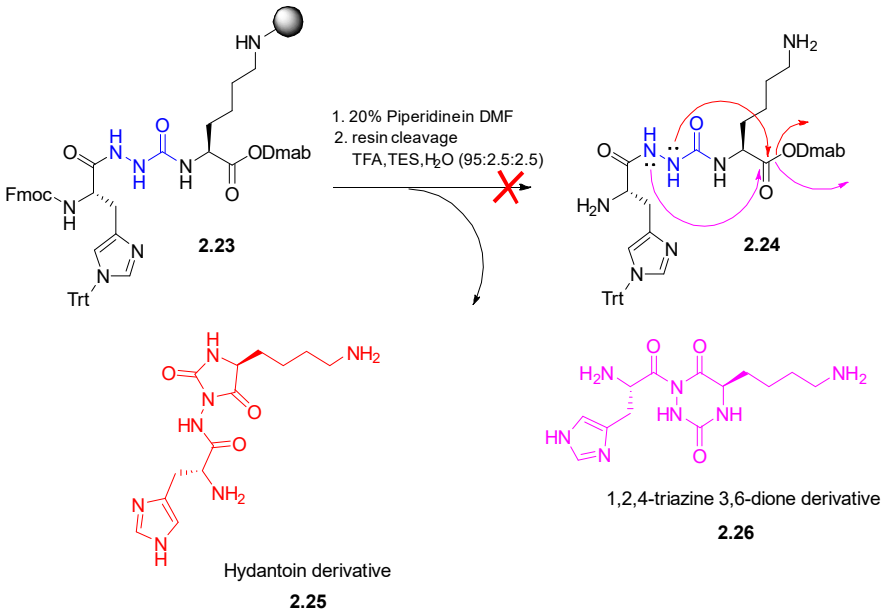

Attempts failed to synthesize [azaG^2]-**CP-2** (**2.2**) using Method I. Carbazate **2.10** could be coupled to the lysine residue. After Fmoc removal and coupling of Fmoc-His(Tr)-OH, azatripeptide **2.23** was observed as a peak at 8.224 retention time in the HPLC chromatogram exhibiting the expected molecular ion (547 m/z). Removal of the Fmoc group from the histidine residue of **2.23** caused intramolecular cyclization with loss of HO-Dmab. After cleavage of the product from loss of the ester protection, analysis by ^{1}H and ^{13}C NMR spectroscopy and mass spectrometry indicated an intramolecular attack of one of the two hydrazine nitrogen to provide

either hydantoin **2.25** or 1,2,4-triazene-3,6-dione **2.26** (Scheme 2.4). Related heterocycles have previously resulted from intramolecular cyclization of aza-glycinates in solution.[13] Considering that protection of the α-nitrogen of the aza-glycine residue as described below avoided cyclization, hydantoin **2.25** was more likely formed. Ring formation to give the *N*-alkyl counterpart of 1,2,4-triazene-3,6-dione **2.26** would have likely been accelerated by an aza-equivalent of the Thorpe-Ingold effect.[14]

Scheme 2.5: Synthesis of [azaG^2]-**CP-2 (2.2)** and (*R*)- and (*S*)-[aza(*i*-PrO)F^2]-**CP-2** [(*R*)- and (*S*)-**2.32**]

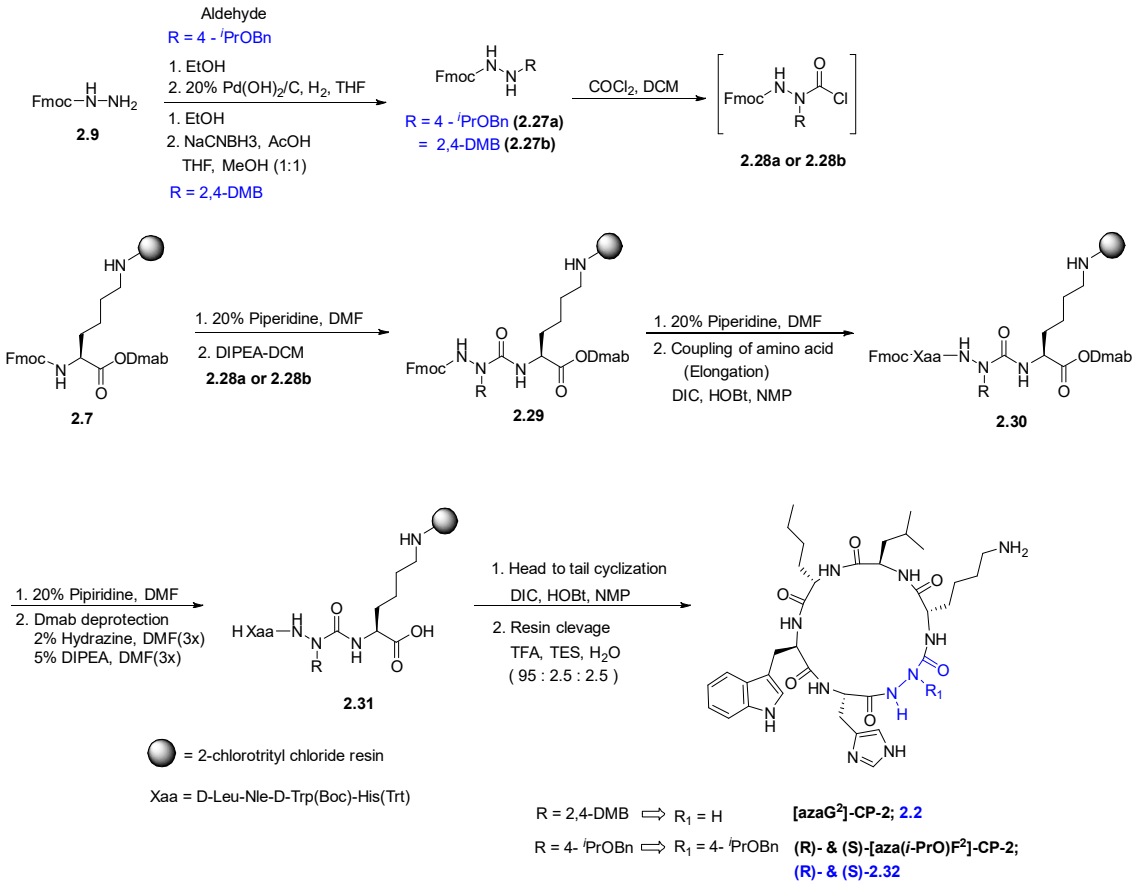

To prevent the intramolecular cyclization in the synthesis of [azaG^2]-**CP-2** (**2.2**), Method II was developed employing protection of the α-nitrogen of the aza-glycine residue (Scheme 2.5).

Alkylation of *N*-(Fmoc)hydrazine **2.9** was accomplished by reductive amination using hydrogenation of the imine generated with 4-isopropoxybenzaldehyde employing palladium-on-carbon, and by hydride reduction of the iminium ion formed with 2,4-dimethoxy benzaldehyde utilizing sodium cyanoborohydride and acetic acid. 4-Isopropoxybenzyl and 2,4-dimethoxy benzyl carbazates **2.27a** and **2.27b** were respectively isolated in 76% and 94% yields from the reductive amination protocols. Carbazates **2.27a** and **2.27b** were respectively activated using phosgene in toluene to give their corresponding substituted aza-phenylalanine acid chlorides **2.28**, which were coupled to lysine resin **2.7** to yield aza-dipeptide resins **2.29**.[10, 15] After Fmoc group removal, azapeptide **2.29** was elongated using protocols described above for [azaG^5]-**CP-2** (**2.5**) employing Fmoc-His(Tr)-OH, Fmoc-D-Trp(Boc)-OH, Fmoc-Nle-OH and Fmoc-D-Leu-OH. Similarly, Fmoc and Dmab group removal, cyclization on resin and cleavage of the solid support with concomitant removal of the side chain protecting groups, all were performed as described for azacyclopeptide **2.5**.

The 4-isopropoxybenzyl group was however not removed under the final TFA treatment and [aza(*i*-PrO)F^2]-**CP-2** was isolated by reverse phase HPLC, which provided two related products having the same desired mass and assumed to be diastereomers due to epimerization at the histidine residue during the coupling reaction. The isomers {e.g., (*R*)- and (*S*)-[aza(*i*-PrO)F^2]-**CP-2** [(*R*)- and (*S*)-**2.32**]} were separated and examined for biological activity. Alternatively, the more acid labile 2,4-dimethoxy benzyl group was successfully removed under the resin-cleavage conditions to provide [azaG^2]-**CP-2** (**2.2**) after purification by reverse-phase HPLC.

Scheme 2.6: General synthetic scheme for preparation of azacyclopeptides **2.1** and **2.6** (Method III)

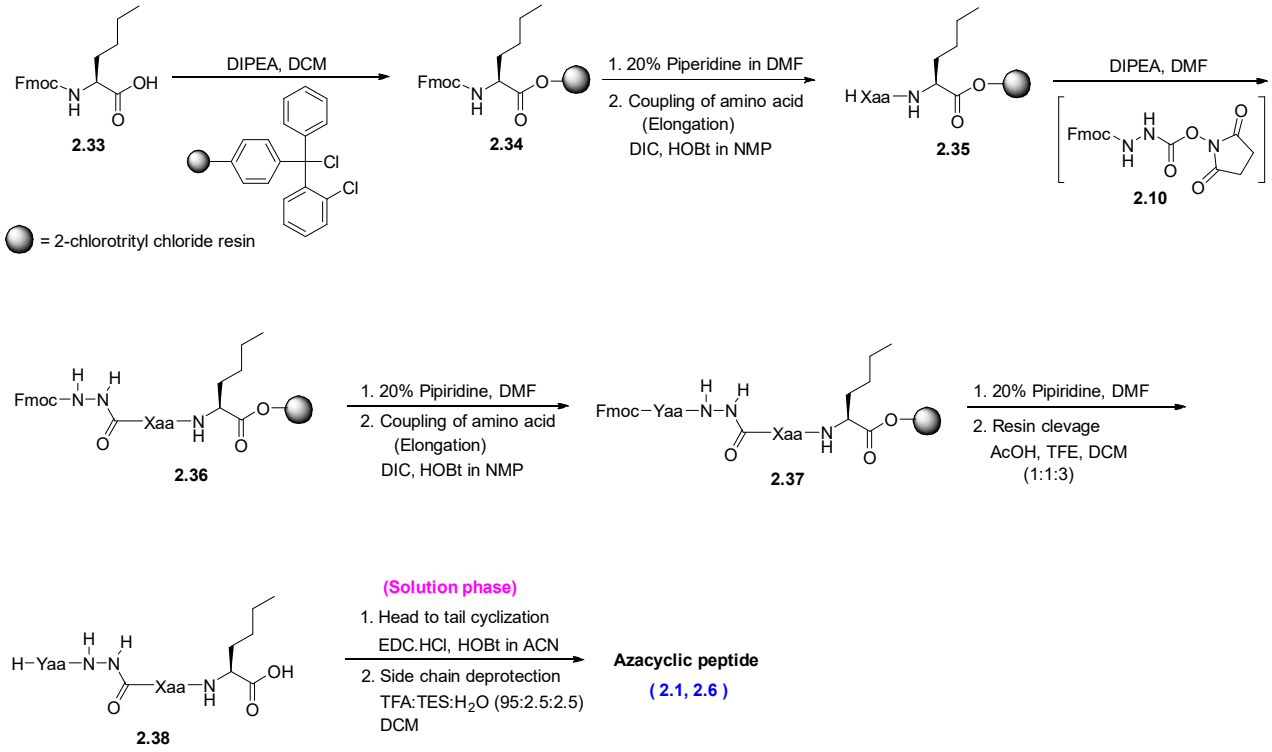

Xaa	Yaa	Cyclicpeptide
D-Leu	D-Trp(Boc)-His(Trt)-D-Ser(tBu)	**[azaG^1]-CP-2 (2.1)**
H	D-Trp(Boc)-His(Trt)-D-Ser(tBu))-Lys	**[azaG^6]-CP-2 (2.6)**

Preparation of [azaG^1]-**CP-2** (**2.1**) in which lysine is replaced by aza-glycine required an alternative approach to anchor the linear sequence to the solid support. Moreover, the synthesis of [azaG^6]-**CP-2** (**2.6**) by Method I would entail intramolecular cyclization by coupling onto a less nucleophilic semicarbazide. An alternate protocol (Method III) was thus employed to synthesize both [azaG^1]-**CP-2** (**2.1**) and [azaG^6]-**CP-2** (**2.6**) (Scheme 2.6). The linear azapeptide sequences were first synthesized on solid support. After resin cleavage without side chain removal,

cyclization in solution was used to prepare the azacyclopeptides, from which the side chain protection was finally removed.

After anchoring Fmoc-Nle-OH **2.33** to 2-chlorotritylchloride resin using *N*,*N*'-didisopropylethylamine,[16] the aza-glycine residue was coupled as active carbazate **2.10** to provide aza-peptide **2.36**. Sequence elongation was performed with DIC, HOBt in NMP and standard solid phase protocols using Fmoc-Leu-OH, Fmoc-Lys(Boc)-OH, Fmoc-D-Ser(*t*-Bu)-OH, Fmoc-His(Tr)-OH and Fmoc-D-Trp(Boc)-OH, respectively. The Fmoc group was removed from the final linear azapeptide **2.37** by agitating the resin with 20% piperidine in DMF. The resin was cleaved using a 1:1:3 mixture of AcOH:TFE:DCM. This mild acid cocktail cleaved successfully the resin without removal of the side chain protection.[17-18] Macrocyclization was performed in solution using EDC•HCl and HOBt in acetonitrile. Side chain protection was finally removed with a 50% solution of TFA:TES:H_2O (95:2.5:2.5) in DCM, and azacyclopeptides **2.1** and **2.6** were purified by reverse phase HPLC. The cyclic azapeptides were characterized by HRMS and demonstrated to be of high purity by RP-HPLC in two different solvent systems (Table 2.1).

Table 2.1. Retention times, purity, and mass spectrometric analyses of azacyclopeptides

Azacyclopeptide	Method	RT[a] (min) MeCN	RT[a] (min) MeOH	purity 214 nm	[M + 1] or [M + 23] ions	
					m/z (calcd)	m/z (obsvd)
[azaG[1]]-**CP-2** (**2.1**)	III	7.19	7.71[b]	>99	695.3624	695.3634
[azaG[2]]-**CP-2** (**2.2**)	II	6.35	6.57[b]	>99	736.4253	736.4263
[azaG[3]]-**CP-2** (**2.3**)	I	7.26	5.88[c]	>95	686.3884	686.3995
[azaG[4]]-**CP-2** (**2.4**)	I	4.38[d]	5.87[e]	>99	637.3780	673.3782
[azaG[5]]-**CP-2** (**2.5**)	I	3.83	4.69	>99	710.3733	710.3740
[azaG[6]]-**CP-2** (**2.6**)	III	4.88	6.56	>99	710.3733	710.3747
(*R*)-[aza(*i*-PrO)F[2]]-**CP-2** (**2.32**)[f]	II	6.92	7.68[b]	>95	884.5141	884.5171
(*S*)-[aza(*i*-PrO)F[2]]-**CP-2** (**2.32**)[f]		7.17	7.97[b]	>97	906.4961	906.4953

Unless otherwise noted, analytical HPLC analyses were performed on a XTerra column from Waters (2.1 mm × 50 mm, 3.5 μm, C18) with a flow rate of 0.5 mL/min using gradients of [a]5-50% CH_3CN [(0.1% formic acid (FA)] in water (0.1% FA) or [a]5-50%, [b]10–90%, or [c]30–95%

MeOH (0.1% FA) in water (0.1% FA), or on an Atlantis column (3.9 mm × 100 mm, 3.5 µm, C18) with a flow rate of 0.5 mL/min using a gradient of [d]20-90% CH_3CN (0.1% FA) in water (0.1% FA) or [e]10−90% MeOH (0.1% FA) in water (0.1% FA). [f](*R*)- and (*S*)-were assigned arbitrarily to **2.32** having the shortest and longest retention times.

Scheme 2.7: Representative scheme for preparation of compound **2.5**

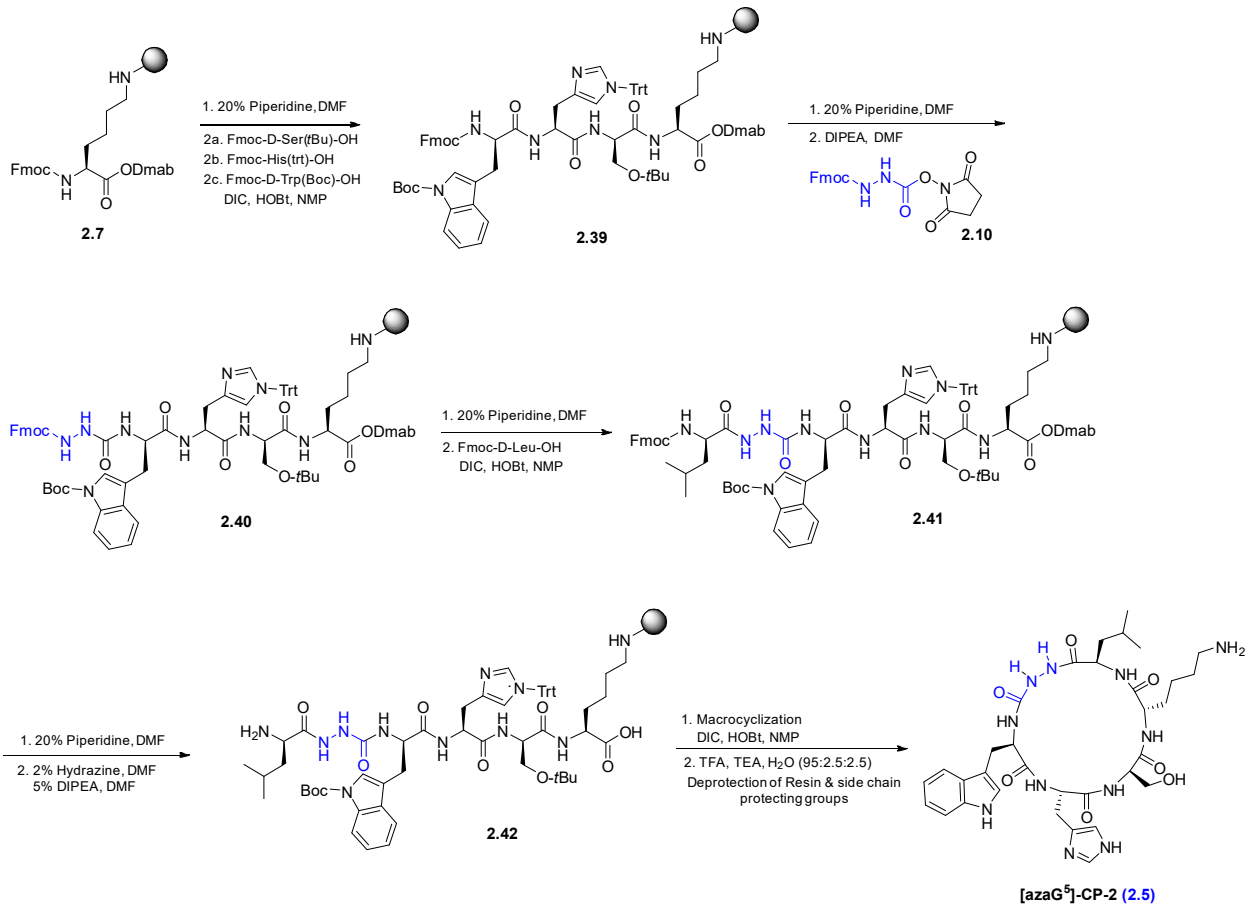

2.3. Biological Assays:

Three different types of assays are planned to evaluate the activity of the [azaG]-**CP-2** analogs. The thioflavin T (ThT) assay is used to assess anti-amyloidogenic activity. A cell viability assay is employed to ascertain neuroprotective activity. Finally, the CMC assay is used to examine self-assembly which may reflect potential to interfere with the aggregation of Aβ to form amyloid.

2.3.1. Thioflavin T aggregation assay

Amyloid generation which is characteristic of diseases such as Alzheimer's and Parkinson's diseases, may be identified and quantified using the thioflavin T fluorescence dye assay.[19-20] Thioflavin T is a benzothiazole salt, which binds to amyloid aggregates. On binding enhanced fluorescence is observed in the emission spectrum.[21]

2.3.2. Neuroprotective activity on Aβ aggregation in cell culture (MTT assay)

Cell-based assays are often used to identify the cytotoxic effect. Cell death may be measured by colorimetry. Tetrazolium salts have been used to detect viable cells. For example, MTT (3-(4,5-dimethylthiazol-2-yl)-2,5-diphenyltetrazolium bromide (MTT) is positively charged and readily penetrates viable eukaryotic cells. The colorimetric MTT assay can measure homogeneous cell viability in a 96-well format suitable for high throughput screening.[22] Viable cells reduce MTT through active metabolism into a purple colored formazan product with absorbance maximum near 570 nm (Figure 2.3).[22-23] Dead cells lose the ability to convert MTT into formazan. The quantity of formazan is directly proportional to the number of viable cells and measurable over time by recording changes in absorbance using spectrophotometer.

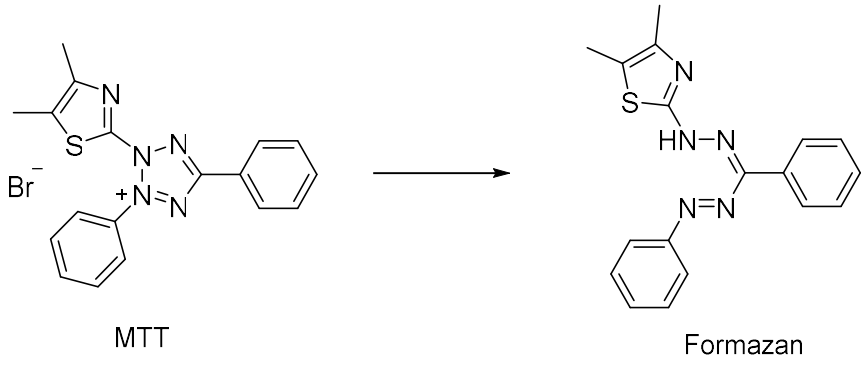

Figure 2.3: Reduction of MTT into formazan derivative

Neurons are highly susceptible to the lethal effects of misfolded proteins which are likely to aggregate at increased concentration.[24] The pheochromocytoma (PC12) cell line is commonly used in *in vitro* studies to examine neuronal variation and neurotoxicity as a model of neurodegenerative disease.[25]

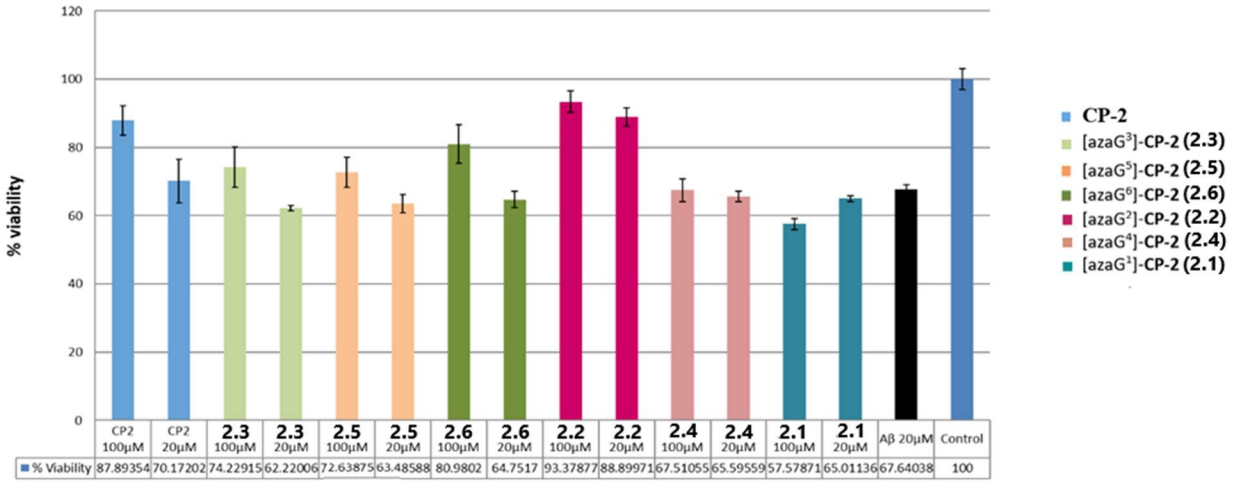

Figure 2.4: Azacyclo-D,L-α-peptide effects on Aβ-induced toxicity in PC12 cells. Aβ40 (20 μM) was aged in the absence or presence of increasing concentrations of azacyclopeptide for 48 h and exposed to PC12 cells for 24 h, when cell viability was determined by the MTT assay.

Employing the MTT assay using a PC12 cell line susceptible to Aβ toxicity (Aβ40 at 20 μM),[26] the [azaG]-**CP-2** series was examined. Notably, [azaG^2]-**CP-2** (**2.2**) in which D-serine was replaced by aza-glycine gave a higher absorbance than lead peptide **CP-2** at both 100 μM and 20 μM concentrations. On the other hand, the other [azaG]-**CP-2** analogs exhibited relatively weaker absorbance relative to **CP-2**. In the model of Aβ-induced toxicity, cyclic azapeptide **2.2** exhibited notable capacity to improve cell viability.

2.3.3. Critical micelle concentration test

Concentration is a key parameter for characterizing self-assembling systems. Critical concentration is defined as the minimum concentration of molecules at which the micelle formation occurs. Certain molecules have two distinct hydrophilic and hydrophobic components with differing affinity for solvents and are said to be amphiphilic in nature. Amphiphilic molecules display distinct behavior when interacting with different solvents. Biomaterials like proteins and self assembling peptides may have a critical aggregation concentration based on their amphiphilic structures. These amphiphilic biomolecules may aggregate once the concentration is above the critical aggregation concentration. Self-assembly of azacyclicpeptides will be examined to evaluate their critical aggregation concentrations.

In summary, three different approaches were developed to successfully perform an aza-glycine scan of **CP-2** resulting in six [azaG]-**CP-2** analogues. In addition, two diastereomers of [aza(*i*-PrO)F^2]-**CP-2** were isolated. All eight azacyclic peptides were submitted for biological assays to identify the anti-amyloidogenic activity using ThT assay, neuroprotection assay in PC12 cells using the MTT assay, and critical aggregation concentration to evaluate potential for self-assembly. In the completed cell viability assay, one of the aza-glycinyl cyclic-D,L-α-peptides, [azaG^2]**CP-2 (2.2)** prevents the death of PC12 cells suffering from Aβ-induced toxicity relative to the parent peptide **CP-2**. Although further studies are in progress, the latter result validates the application of aza-glycine residues in the study of cyclic-D,L-α-peptides towards the development of new prototypes for therapy to treat amyloid diseases.

2.4 References

1. Zhang, Y.; Malamakal, R. M.; Chenoweth, D. M. Aza-glycine induces collagen hyperstability. *J. Am. Chem. Soc.* **2015,** *137*, 12422-12425.

2. Kasznel, A. J.; Zhang, Y.; Hai, Y.; Chenoweth, D. M. Structural Basis for Aza-Glycine Stabilization of Collagen. *J. Am. Chem. Soc.* **2017,** *139*, 9427-9430.

3. Berthelot, T.; Gonçalves, M.; Laïn, G.; Estieu-Gionnet, K.; Déléris, G. New strategy towards the efficient solid phase synthesis of cyclopeptides. *Tetrahedron* **2006,** *62*, 1124-1130.

4. Chan, W. C.; Bycroft, B. W.; Evans, D. J.; White, P. D. A novel 4-aminobenzyl ester-based carboxy-protecting group for synthesis of atypical peptides by Fmoc-But solid-phase chemistry. *J. Chem. Soc., Chem. Commun.* **1995**, 2209-2210.

5. Johnson, T.; Liley, M.; Cheeseright, T. J.; Begum, F. Problems in the synthesis of cyclic peptides through use of the Dmab protecting group. *J. Chem. Soc., Perkin Trans. 1* **2000**, 2811-2820.

6. Conroy, T.; Jolliffe, K. A.; Payne, R. J. Efficient use of the Dmab protecting group: applications for the solid-phase synthesis of N-linked glycopeptides. *Org. Biomol. Chem.* **2009,** *7*, 2255-2258.

7. Chingle, R.; Proulx, C.; Lubell, W. D. Azapeptide synthesis methods for expanding side-chain diversity for biomedical applications. *Acc. Chem. Res.* **2017,** *50*, 1541-1556.

8. Garcia-Ramos, Y.; Lubell, W. D. Synthesis and alkylation of aza-glycinyl dipeptide building blocks. *J. Pept. Sci.* **2013,** *19*, 725-729.

9. Bourguet, C. B.; Sabatino, D.; Lubell, W. D. Benzophenone semicarbazone protection strategy for synthesis of aza-glycine containing aza-peptides. *Pept. Sci.* **2008,** *90*, 824-831.

10. Gibson, C.; Goodman, S. L.; Hahn, D.; Hölzemann, G.; Kessler, H. Novel solid-phase synthesis of azapeptides and azapeptoides via Fmoc-strategy and its application in the synthesis of RGD-mimetics. *J. Org. Chem.* **1999,** *64*, 7388-7394.

11. Lubell, W.; Blankenship, J.; Fridkin, G.; Kaul, R. (2005) Peptides. *Science of Synthesis 21.11, Chemistry of Amides*. Thieme, Stuttgart, 713-809.

12. Malkinson, J. P.; Zloh, M.; Kadom, M.; Errington, R.; Smith, P. J.; Searcey, M. Solid-phase synthesis of the cyclic peptide portion of chlorofusin, an inhibitor of p53-MDM2 interactions. *Org. Lett.* **2003,** *5*, 5051-5054.

13. Bourguet, C. B.; Proulx, C.; Klocek, S.; Sabatino, D.; Lubell, W. D. Solution-phase submonomer diversification of aza-dipeptide building blocks and their application in aza-peptide and aza-DKP synthesis. *J. Pept. Sci.* **2010,** *16*, 284-296.

14. Jung, M. E.; Piizzi, G. gem-Disubstituent Effect: Theoretical Basis and Synthetic Applications. *Chem. Rev.* **2005,** *105*, 1735-1766.

15. Boeglin, D.; Lubell, W. D. Aza-amino acid scanning of secondary structure suited for solid-phase peptide synthesis with Fmoc chemistry and aza-amino acids with heteroatomic side chains. *J. Comb. Chem.* **2005,** *7*, 864-878.

16. Athanassopoulos, P.; Barlos, K.; Gatos, D.; Hatzi, O.; Tzavara, C. Application of 2-chlorotrityl chloride in convergent peptide synthesis. *Tetrahedron Lett.* **1995,** *36*, 5645-5648.

17. Barlos, K.; Gatos, D.; Kallitsis, J.; Papaphotiu, G.; Sotiriu, P.; Wenqing, Y.; Schäfer, W. Darstellung geschützter peptid-fragmente unter einsatz substituierter triphenylmethyl-harze. *Tetrahedron Lett.* **1989,** *30*, 3943-3946.

18. Barlos, K.; Chatzi, O.; Gatos, D.; Stavropoulos, G. 2-chlorotrityl chloride resin. *Int. J. Pept. Protein Res.* **1991,** *37*, 513-520.

19. Xue, C.; Lin, T. Y.; Chang, D.; Guo, Z. Thioflavin T as an amyloid dye: fibril quantification, optimal concentration and effect on aggregation. *Royal Soc. Open Sci.* **2017,** *4*, 160696.

20. Biancalana, M.; Koide, S. Molecular mechanism of Thioflavin-T binding to amyloid fibrils. *Biochim. Biophys. Acta, Proteins Proteomics* **2010,** *1804*, 1405-1412.

21. Groenning, M. Binding mode of Thioflavin T and other molecular probes in the context of amyloid fibrils—current status. *J. Chem. Biol.* **2010,** *3*, 1-18.

22. Mosmann, T. Rapid colorimetric assay for cellular growth and survival: Application to proliferation and cytotoxicity assays. *J. Immunol. Methods* **1983,** *65*, 55-63.

23. Marshall, N.; Goodwin, C.; Holt, S. A critical assessment of the use of microculture tetrazolium assays to measure cell growth and function. *Growth Regul.* **1995,** *5*, 69-84.

24. Taylor, J. P.; Hardy, J.; Fischbeck, K. H. Toxic proteins in neurodegenerative disease. *Science* **2002,** *296*, 1991-1995.

25. Westerink, R.; Ewing, A. The PC12 cell as model for neurosecretion. *Acta Physiol.* **2008,** *192*, 273-285.

26. Mozes, E.; Hunya, A.; Posa, A.; Penke, B.; Datki, Z. A novel method for the rapid determination of beta-amyloid toxicity on acute hippocampal slices using MTT and LDH assays. *Brain Res. Bull.* **2012,** *87*, 521-525.

Chapter 3: Conclusion and perspectives

3.1. Conclusion and perspectives:

An aza-glycine scan of the anti-amyloidogenic cyclic peptide **CP-2** was accomplished by way of four methods for azapeptide assembly. In addition, two [aza(*i*-PrO)F^2]-**CP-2** analogs were synthesized. All eight azacyclopeptides were submitted for *in vitro* studies.

At present, their cytoprotective effects have been assessed in PC12 cells using the MTT assay. Furthermore, their anti-aggregation activity and critical micelle concentrations are under study. Although the majority of analogues were not as potent as the lead peptide **CP-2** in the cell viability assay MTT, the azacyclicpeptide in which D-serine was replaced by aza-glycine, [azaG^2]-**CP-2** (**2.2**) exhibited improved absorbance compared to the parent peptide indicating greater potential to prevent the death of cells suffering from Aβ toxicity.

The preliminary results obtained with [azaG^2]-**CP-2** (**2.2**) merit further investigation. In the future, the thioflavin T (ThT) assay will be performed to assess anti-amyloidogenic activity. The propensity of the azaGly-peptides to self-assemble will be studied using a critical micelle concentration test, in which the hydrophilic and hydrophobic parts of the molecules may play important roles. These assays will further evaluate the self-assembly propensity of the azacyclic D,L-α-peptides to generate supramolecular structures and their anti-amyloidogenic activity. Finally, conversion of [azaG^2]-**CP-2** (**2.2**) into a radio-tracer may provide a tool for measuring early Aβ oligomer formation using PET imaging.

Annex 1: Experimental part of Chapter 2

Materials & Methods:

2-Chlorotrityl chloride resin (0.79 mmol/g or 1.14 mmol/g) was purchased from Chem-Impex Int'l Inc., and the manufacturer's reported loading of the resin was used in the calculation of the yields of the final products. The 20% solution of phosgene in toluene was purchased from Aldrich. Unless otherwise mentioned, all reagents from commercial sources were used as received. Dry solvents (DCM, DMF and THF) were obtained by passage through solvent filtration systems (Glass Contour Irvine, CA). Ethanol, ethyl acetate, and methanol were obtained from Fisher Chemical. Melting points are uncorrected, reported in degree Celsius (°C), and obtained on a sample that was placed in a capillary tube using a Gallen Kamp melting point apparatus equipped with a thermometer. ^{1}H and ^{13}C NMR spectra were recorded at room temperature (298 K) in DMSO-*d*6 (2.50 ppm/39.52 ppm) on Bruker AV (400/100 and 500/125 MHz) instruments and referenced to internal solvent. Chemicals shifts are reported in parts per million (ppm) and coupling constants (*J* values) are reported in Hertz. The abbreviations for peak multiplicities are s (singlet), d (doublet), t (triplet), dd (doublet of doublet), m (multiplet), and br (broad). Low resolution mass spectrometric analyses were performed on a LCMSD instrument from Agilent Technologies in positive electrospray ionization mode (ESI+). High resolution mass spectrometry (HRMS) data were obtained by the Regional Center for Mass Spectrometry at the Université de Montreal. Purity was ascertained using analytical HPLC, which was performed on a Xterra reverse-phase column from Waters (2.1 mm × 50 mm, 3.5 μm, C18) or an Atlantis reverse phase column from Waters (3.9 mm × 100 mm, 3.5 μm, C18) with a flow rate of 0.5 mL/min using a gradient of acetonitrile (0.1% formic acid) or methanol (0.1% formic acid) in water (0.1% formic acid). All the Azacyclopeptides tested for biological activity presented purity of ≥ 95%.

[azaG^5]-CP-2 (2.5):

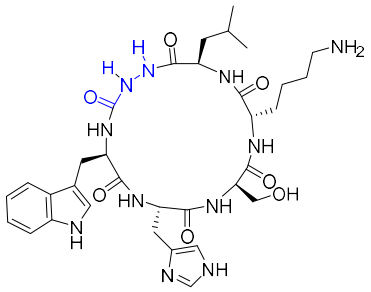

Resin **2.39** was synthesized starting from Fmoc-Lys-ODmab resin **2.7** (0.32 mmol) by sequential Fmoc deprotections with 20% piperidine in DMF, and couplings using Fmoc-D-Ser(O^{t}Bu)-OH, Fmoc-His(Trt)-OH and Fmoc-D-Trp(Boc)-OH with DIC (3 eq.) and HOBt (3 eq.) in NMP according to the general protocol. The resin aliquot was cleaved as described above using TFA/TES/H_2O (95:2.5:2.5) and analyzed by UV-HPLC which indicated Fmoc-D-Trp-His-D-Ser-Lys-ODmab was of approximately 70% purity: RT 9.00 min on Sunfire column using a gradient of 5-50% MeCN (0.1%) in water (0.1%) over 8 min. After removal of the Fmoc group from resin **2.39**, the peptide was treated with active carbazate **2.10** as described below.

A solution of DSC (3 eq., 246 mg, 0.96 mmol) in dry DMF (4 mL) was treated dropwise with a solution of Fmoc hydrazine **2.9** (3 eq., 248 mg, 0.96 mmol) in dry DMF (5 mL) over 10-15 min at 0 °C under inert atmosphere. The reaction mixture was stirred at room temperature for 1 h and transferred to a syringe tube equipped with a Teflon™ filter, stopper and stopcock containing Fmoc deprotected resin **2.39** (1 eq., 600 mg, 0.32 mmol) in DMF (4 mL). The resin mixture was then treated with DIPEA (6 eq., 0.33 mL, 1.92 mmol), shaken on an automated shaker for 14-16 h, and filtered. After filtration, the resin washed sequentially with DMF (3x), MeOH (3x) and DCM (3x), and dried under vacuum, to afford the aza-glycine resin **2.40**. Analysis of an aliquot of resin **2.40** by HPLC indicated the absence of the starting material and Fmoc-aza-Gly-D-

Trp-His-D-Ser-Lys-ODmab of 50% purity was observed at RT 8.9 min, on Sunfire column with a gradient of 5-50% MeCN (0.1% FA) in water (0.1% FA) over 14 min.

After removal of the Fmoc group from azapeptide **2.40**, amide coupling was continued with Fmoc D-Leu-OH using DIC (3 eq.) and HOBt (3 eq.) in NMP yielded to provide azapeptide **2.41**. Analysis of an aliquot of resin **2.41** by HPLC indicated formation of Fmoc-D-Leu-aza-Gly-D-Trp-His-D-Ser-Lys-ODmab at RT 9.3 min on Sunfire column with a gradient of 5-50% MeCN (0.1% FA) in water (0.1% FA) over 14 min.

After the Fmoc and Dmab groups were removed from resin **2.41**, the resin washed with DMF (3x), MeOH (3x) and DCM (3x) in sequence and dried to provide azapeptide resin **2.42**. ES-MS Analysis of resin aliquot **2.42,** confirmed the desired product with m/z = 728.47. The head to tail cyclization of the linear peptide on resin **2.42** (1 eq., ~550 mg, 0.32 mmol) was performed using DIC (3 eq.) and HOBt (3 eq.) in NMP for 16 h (2x). The resin was washed, dried, and treated with 10 mL of a freshly made solution of TFA/TES/H_2O (95:2.5:2.5) for 2 h. The resin was filtered and washed with TFA (10 mL). The combined filtrate and washing mixture was concentrated to a residue, that was triturated with diethyl ether to give light-yellow solid, which was purified by reverse phase HPLC on a Gemini® C18 column (Phenomenex® Inc., pore size: 110 Å, particle size: 5µm, 250x21.2 mm) using a binary solvent system consisting of a gradient of 10% - 60% MeCN (0.1% FA) in water (0.1% FA), with flow rate of 10 mL/min, and UV detection at 214 nm. The desired fractions were combined and freeze dried to give 9.2 mg (4% yield) cyclic azapeptide [azaG^5]-CP-2 **(2.5)** as white fluffy solid: analytical RP-HPLC on XTerra^{TM} column 3.5µm (2.1 x 50 mm) using a gradient of 5-50% MeCN (0.1% FA) in water (0.1% FA) over 8 min, with 99.87% purity at RT = 3.83; gradient of 5-50% MeOH (0.1% FA) in water (0.1% FA) over 8 min, with 99.55% purity at RT = 4.69; HRMS m/z calcd. For $C_{33}H_{48}N_{11}O_7$ $[M+H]^+$ 710.3733, found

710.3740. Employing modifications of the protocol described for the synthesis of [azaG^5]-CP-2 **(2.5),** [azaG^3]-CP-2 **(2.3),** and [azaG^4]-CP-2 **(2.4)** were synthesized respectively in 2% and 4% yields.

[azaG^2]-CP-2 (2.2):

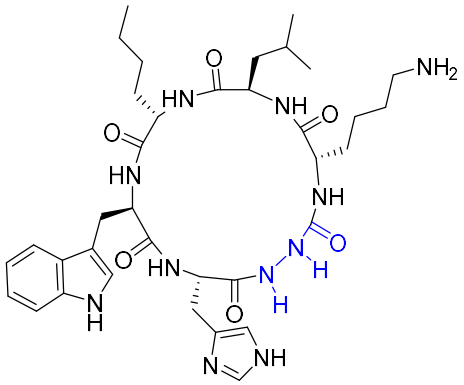

To a solution of *N*-fluorenylmethyl-*N'*-(2,4-dimethoxybenzyl) carbazate (**2.27b**, 3 eq., 364 mg, 0.90 mmol) in dry DCM (10 mL) under inert atmosphere at 0 °C, a solution of phosgene in toluene (20% w/v, 6 eq., 0.83 mL, 1.8 mmol) was added dropwise. After complete consumption of the starting carbazate was observe by TLC (generally 15-30 min), the reaction mixture was concentrated under reduced pressure. The residue containing acid chloride **2.28** was dissolved in dry DCM (10 mL), treated with DIPEA (12 eq., 0.63 mL, 3.6 mmol), and transferred to a syringe tube equipped with a Teflon™ filter, stopper and stopcock containing resin Fmoc-Lys-ODmab **2.7** (1 eq., 0.3 mmol) swollen in DCM (5 mL). The swollen resin mixture was shaken on an automated shaker for 12 h, filtered, washed, and dried to get resin **2.29,** which was confirmed by ES-MS analysis (m/z = 560) of aliquot of resin cleaved and UV-HPLC shows absence of starting material and observed a prominent peak. Aza-glycine resin **2.29** was elongated, cyclized, and cleaved using the same protocols as described for the synthesis of [azaG^5]-**CP-2** (**2.5**) above. The crude product was purified by reverse phase HPLC on a Gemini® C18 column (Phenomenex® Inc., pore size: 110 Å, particle size: 5µm, 250x21.2 mm) using a binary solvent system consisting of a gradient of

10% - 60% MeCN (0.1% FA) in water (0.1% FA), with flow rate of 10 mL/min, and UV detection at 214 nm. The desired fractions were combined and freeze dried to give 9.0 mg (4% yield) cyclic azapeptide [azaG^2]-**CP-2 (2.2)** as white fluffy solid: analytical RP-HPLC on XTerra^{TM} column 3.5µm (2.1 x 50 mm) using a gradient of 5-50% MeCN (0.1% FA) in water (0.1% FA) over 8 min, with >99 % purity at RT = 6.353; gradient of 10-90% MeOH (0.1% FA) in water (0.1% FA) over 9 minwith >99 % purity at RT = 6.573; HRMS m/z calcd. For $C_{36}H_{54}N_{11}O_6$ $[M+H]^+$ 736.4253, found 736.42627.

Following the same protocol described for the synthesis of [azaG^2]-**CP-2 (2.2),** *N*-fluorenylmethyl-*N'*-(4-isopropoxybenzyl) carbazate **(2.27a)** used for the introduction aza residue into peptide backbone resulted (*R*) and (*S*)-[aza(*i*-PrO)F^2]-**CP-2** (**2.32**) 1.3 mg and 1.5 mg (1.3 % over all yield) of >97 % purity.

***N*-Fluorenylmethyl-*N'*-(2,4-dimethoxybenzyl)carbazate (2.27b):**

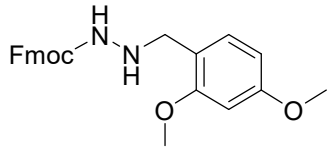

A suspension of *N*-(Fmoc) hydrazine (**2.9,** 1 eq., 1 g, 3.93 mmol) in EtOH (30 mL) was treated with 2,4-dimethoxybenzaldehyde (1.25 eq., 0.82 g, 4.92 mmol), heated at reflux for 2 h, cooled to room temperature, and filtered. The solid was washed with hexane (10 mL), dried under reduced pressure, dissolved in 100 mL of 1:1 THF/MeOH, treated with and $NaBH_3CN$ (1.5 eq., 0.37 g, 5.90 mmol) followed by AcOH (2 mL), and heated at 50 °C for 14 h. The reaction was monitored by ES-MS. The mixture was concentrated in *vacuo*. The residue was dissolved in EtOAc, washed with water and brine, dried over Na_2SO_4, and concentrated under reduced pressure and the residue was recrystallised from hexane (30 mL). The precipitate was stirred for 10 min and filtered, and dried under reduced pressure. Carbazate **2.27b** (900 mg, 57% yield) was isolated as off-white solid.

mp 128-130 °C, ^{1}H NMR (400 MHz, DMSO-d_6) δ 8.71 (br s, 1H), 7.90−7.88 (d, J = 8.0 Hz, 2H), 7.70-7.69 (d, J = 4 Hz, 2H), 7.44-7.40 (t, J = 8 Hz, 2H), 7.34-7.30 (t, J = 8 Hz, 2H) 7.20-7.18 (d, J = 8 Hz, 1H), 6.52 (s, 1H), 6.47-6.45 (d, J = 8 Hz, 1H), 4.69 (br s, 1H), 4.31-4.30 (d, J = 4 Hz, 2H), 4.23-4.21 (d, J = 8 Hz, 1H), 3.85 (br s, 2H), 3.80 (s, 6H); ^{13}C NMR (100 MHz, DMSO-d_6) δ 159.77, 158.31, 156.90, 143.90, 140.81, 130.24, 127.71, 127.14, 125.35, 120.18, 118.64, 104.30, 98.27, 65.62, 55.39, 55.21, 46.80, 30.51; HRMS (ESI+): m/z for $C_{24}H_{25}N_2O_4$ $[M + H]^+$ calcd. 405.1809, found 405.1808 and $C_{24}H_{24}N_2O_4Na$ $[M + Na]^+$ calcd. 427.1628, found 427.1637.

_N_-Fluorenylmethyl-_N'_-(4-_iso_-propoxybenzyl)carbazate (2.27a):

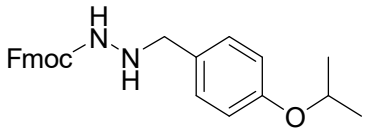

A suspension of _N_-(Fmoc)hydrazine (**2.9**, 1 eq., 600 mg, 2.36 mmol) in EtOH (20 mL) was treated with 4-_iso_-propoxybenzaldehyde (1.25 eq., 485 mg, 2.95 mmol), heated at reflux for 2 h, cooled to room temperature and filtered. The solid was washed with hexane (10 mL), dried under reduced pressure, dissolved in THF (25 mL), and placed into a sealable tube containing a screw cap. Under argon atmosphere, the solution was treated with 20 wt % palladium hydroxide-on-carbon (0.1 eq., 165 mg, 0.24 mmol). The resulting suspension was stirred under 100 psi hydrogen atmosphere for 16 h. The reaction was monitored by ES-MS. The reaction mixture was filtered on Celite™ and washed with methanol. The filtrate and washings were combined and concentrated in vacuo. The resulting white solid was suspended in hexane (20 mL), stirred for 10 min and filtered, dried under vacuum to provide carbazate **2.27a** (1.2 g, 76%) as white solid. mp 107-110 °C, ^{1}H NMR (400 MHz, DMSO-d_6) δ 8.69 (br s, 1H), 7.90−7.88 (d, J = 7.36 Hz, 2H), 7.70-7.68 (d, J = 6.28 Hz, 2H), 7.44-7.40 (dd, J = 7.16, 7.08 Hz, 2H), 7.34-7.30 (dd, J = 7.24, 7.04 Hz, 2H) 7.20 (br s, 2H), 6.85-6,83 (d, J = 7.8 Hz, 2H), 4.81 (br s, 1H), 4. 57-4.53 (m, 1H), 4.32 (br s, 2H), 4.22 (br s, 1H), 3.82

(br s, 2H), 1.25 – 1.23 (d, J = 5.72 Hz, 6H); ^{13}C NMR (100 MHz, DMSO-d_6) δ 157.31, 156.94, 144.28, 141.21, 130.74, 130.27, 128.09, 127.51, 125.71, 120.56, 115.69, 69.47, 65.91, 54.22, 47.20, 22.31, HRMS (ESI+): m/z for $C_{25}H_{26}N_2O_3Na$ $[M + Na]^+$ calcd. 425.1836, found 425.1846.

[azaG^6]-CP-2 (2.6):

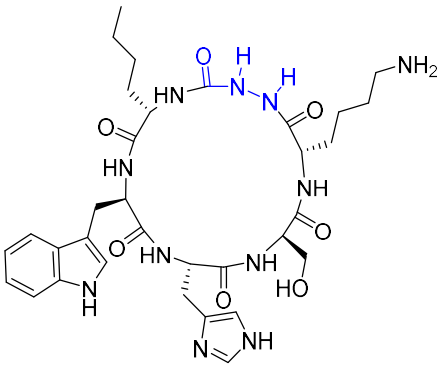

A solution of Fmoc-Nle-OH (**2.33,** 1 eq., 1 g, 2.83 mmol) and DIPEA (3 eq., 1.5 mL, 8.49 mmol) in DCM (20 mL) was added to 2-chlorotrityl chloride polystyrene resin (2.86 g, 0.79 mmol/g), and the mixture was agitated for 16 h. The resin was filtered, washed and dried to provide resin **2.34**. After removal of the Fmoc from **2.34** (0.30 mmol), the norleucine resin was treated with active carbazate **2.10**, that was prepared from *N*-(Fmoc)hydrazine (**2.9**, 3 eq., 229 mg, 0.90 mmol), DSC (3 eq., 231 mg, 0.90 mmol) and DIPEA (6 eq., 0.32 mL, 1.8 mmol) in dry DMF (10 mL). An aliquot of the resulting resin **2.36** was analyzed by ES-MS indicated formation of Fmoc-aza-Gly-Nle-OH and UV-HPLC shows significant peak to go for next step. After Fmoc group removal, azapeptide **2.36** resin was elongated with Fmoc-Lys(Boc)-OH, Fmoc-D-Ser(*t*-Bu)-OH, Fmoc-His(Trt)-OH and Fmoc-D-Trp(Boc)-OH using DIC (3 eq.) and HOBt (3 eq.) in NMP. Cleavage of a resin aliquot and analysis by UV-HPLC and ES-MS indicated formation of Fmoc-D-Trp-His-D-Ser-Lys-aza-Gly-Nle-OH: m/z = 950.53, purity = ~85%, RT = 7.6, HPLC conditions: XTerra^{TM} column 3.5µm (2.1 x 50 mm) using a gradient of 5-50% MeCN (0.1% FA) in water (0.1% FA) over 8 min., After Fmoc group removal from resin **2.37**, treatment with a

mixture of AcOH/TFE/DCM (1:1:3, 10 mL) for 30 min (2x), filtration of the resin and washing, followed by evaporation of the filtrate and washings gave 350 mg of a residue containing azapeptide **2.38**. The residue was dissolved in MeCN (200 mL) , treated with EDC•HCl (173 mg, 0.90 mmol, 3 eq.) and HOBt (122 mg, 0.90mmol, 3 eq.), stirred at room temperature overnight and concentrated to a residue, analysis of which by ES-MS indicated cyclization (m/z = 710.60). The residue was dissolved in DCM (10 mL), treated with 10 mL of a solution of TFA/TES/H_2O (95:2.5:2.5) for 4 h, and concentrated to a residue that was triturated with diethyl ether to provide a light-yellow solid, which was purified by reverse-phase HPLC on a Gemini® C18 column (Phenomenex® Inc., pore size: 110 Å, particle size: 5μm, 250 x 21.2 mm) using a gradient of 10-60% MeCN (0.1% FA) in water (0.1% FA), with flow rate of 6 mL/min, and UV detection at 214 nm. The desired fractions were combined and freeze-dried to provide 13 mg (6% yield) of [azaG^6]-CP-2 (**2.6**) as white fluffy solid: analytical RP-HPLC on XTerra^{TM} column 3.5μm (2.1 x 50 mm) using a gradient of 5-50% MeCN (0.1% FA) in water (0.1% FA) over 8 min, with > 99% purity at RT = 4.88; gradient 2: 5-50% MeOH (0.1% FA) in water (0.1% FA) over 8 min, with > 99% purity at RT = 6.56; HRMS m/z calcd. For $C_{33}H_{48}N_{11}O_7$ $[M+H]^+$ 710.3733, found 710.3747

Employing the protocol described for the synthesis of [azaG^6]-CP-2 (**2.6**), [azaG^1]-CP-2 (**2.1**, 59 mg, 15% yield) was synthesized.

Experimental procedure for Cell culture:[1-2]

Rat pheochromocytoma cells (PC12) were maintained in low glucose Dulbecco's Modified Eagle Medium (DMEM) supplemented with horse serum (HS, 10%) and fetal bovine serum (FBS, 5%), L-glutamine, penicillin, and streptomycin in a 5% CO_2 atmosphere at 37 °C. The effect of the cyclic D,L-α-peptides on Aβ-induced toxicity was evaluated using Aβ40 (20 μM), that was aged for 48 h in the absence or presence of the cyclic peptides (up to a 5-fold mole excess of cyclic D,L-

peptides compared to Aβ in 5% DMSO) in PBS in a total volume of 50 μL. On the day of the experiment, the medium was replaced with fresh medium (90 μL), and the aged samples (10 μL) were then diluted by a factor of 10 in the medium. Control wells received PBS (10 μL) containing 0.25% DMSO (100% cell viability). Cells were incubated for an additional 24 h, and cell viability was then determined by the 3-(4,5-dimethylthiazol-2-yl)-2,5-diphenyltetrazolium bromide (MTT) assay. The absorbance intensity of the Formazan solution was determined at 570 nm using a plate reader.

References:

1. Richman, M.; Wilk, S.; Chemerovski, M.; Wärmländer, S. K.; Wahlström, A.; Gräslund, A.; Rahimipour, S. In vitro and mechanistic studies of an antiamyloidogenic self-assembled cyclic d, l-α-peptide architecture. *J. Am. Chem. Soc.* **2013,** *135*, 3474-3484.

2. Chemerovski-Glikman, M.; Richman, M.; Rahimipour, S. Structure-based study of antiamyloidogenic cyclic d, l-α-peptides. *Tetrahedron* **2014,** *70*, 7639-7644.

Annex 2: HPLC & HRMS spectra for Chapter 2

Analytical HPLC systems for LC-MS characterization of purified cyclic aza-peptides: flow rate of 0.5 mL/min; Methods A-D on XTerra^{TM} reverse-phase column (2.1 mm × 50 mm, 3.5 μm, C18); Methods E-F on Atlantis reverse-phase column (3.9 mm × 100 mm, 3.5 μm, C18).

Method A: 5-50% acetonitrile [0.1% formic acid (FA)] in water (0.1% FA) over 8 min followed by 50% acetonitrile (0.1% FA) in water (0.1% FA) over 1 min.

Method B: 5-50% methanol [0.1% formic acid (FA)] in water (0.1% FA) over 8 min followed by 50% methanol (0.1% FA) in water (0.1% FA) over 1 min.

Methods C and E: 10-90% methanol (0.1% FA) in water (0.1% FA) over 9 min followed by 90% methanol (0.1% FA) in water (0.1% FA) over 1 min.

Method D: 30-95% methanol (0.1% FA) in water (0.1% FA) over 8 min followed by 95% methanol (0.1% FA) in water (0.1% FA) over 1 min.

Method F: 20-90% acetonitrile (0.1% FA) in water (0.1% FA) over 9 min followed by 90% acetonitrile in water (0.1% FA) over 1 min.

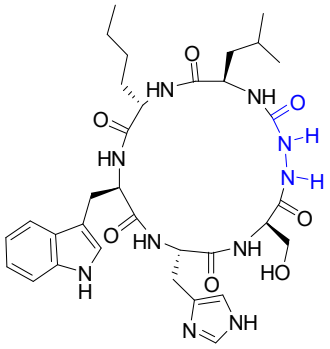

[azaG^1]-CP-2

2.1

a) Method A

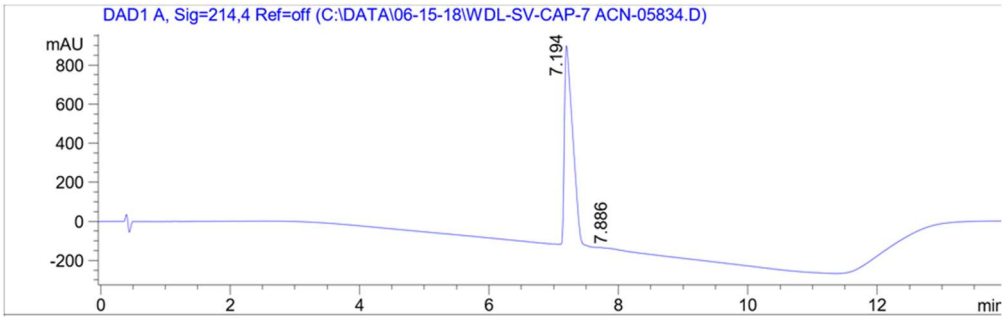

b) Method C

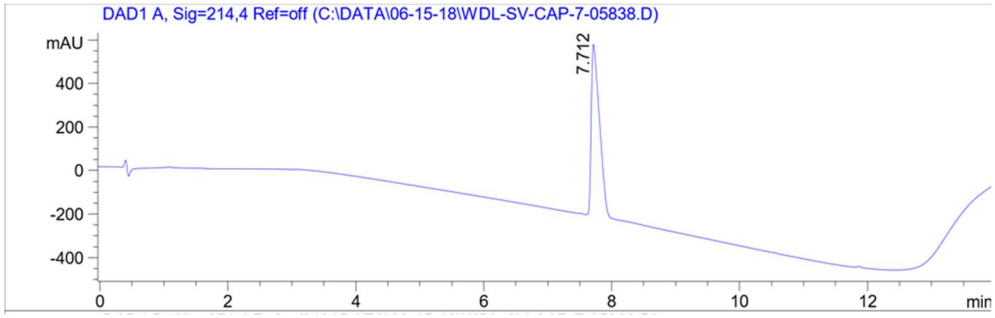

c) HRMS

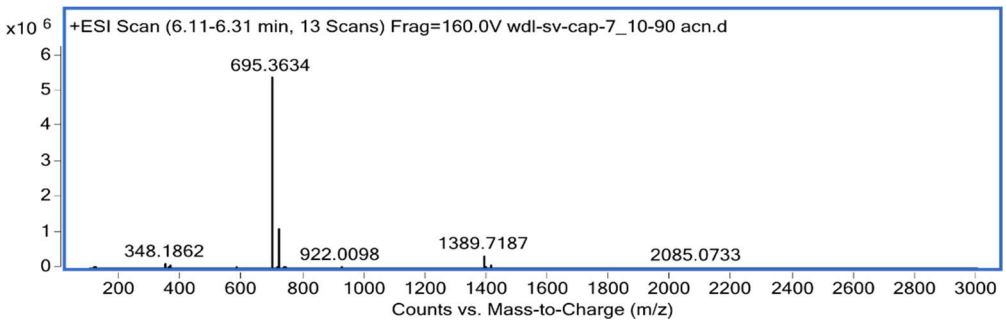

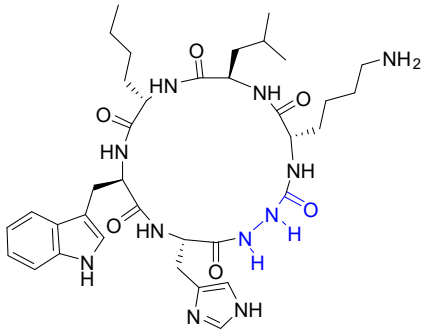

[azaG^2]-CP-2

2.2

a) Method A

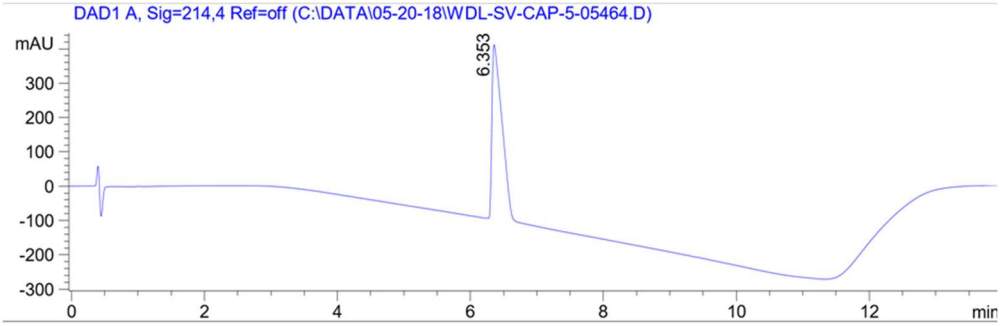

b) Method C

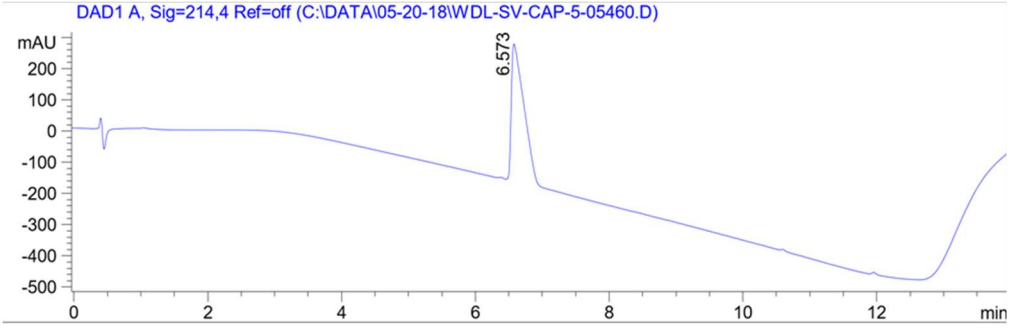

C) HRMS

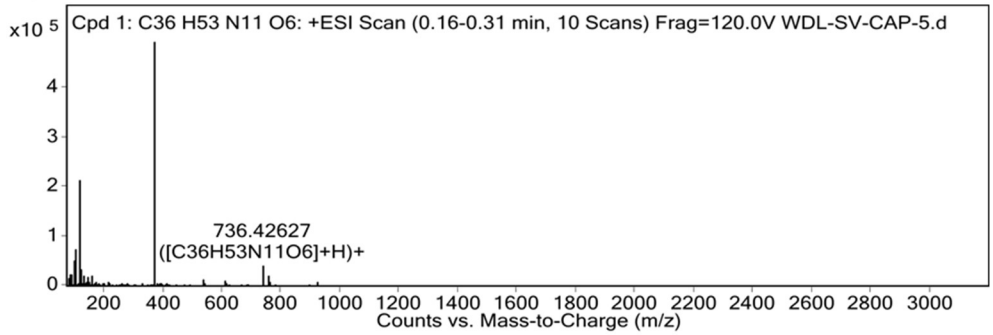

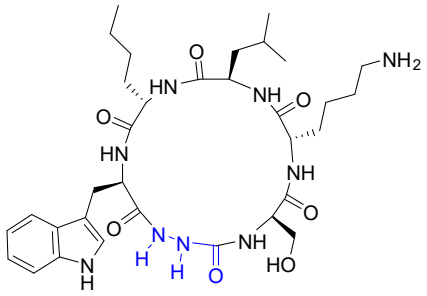

[azaG^3]-CP-2
2.3

a) Method A

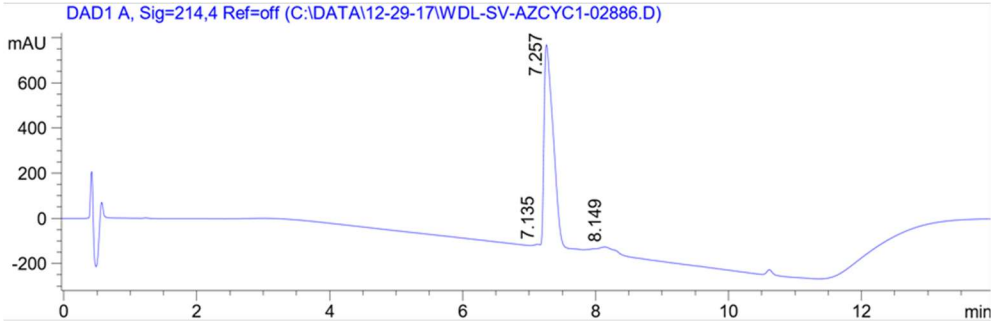

b) Method D

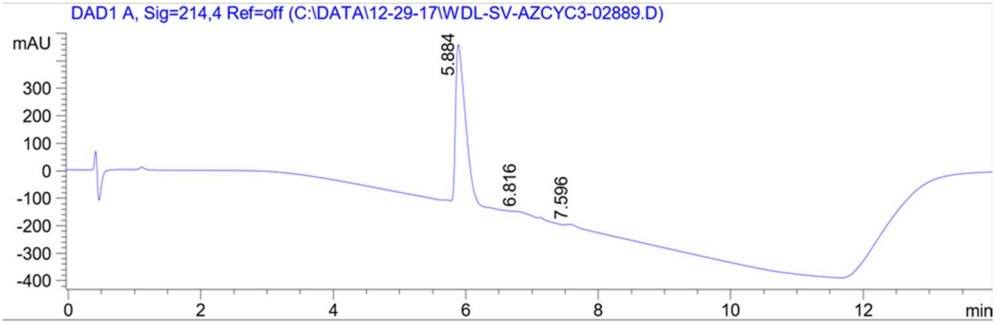

c) HRMS

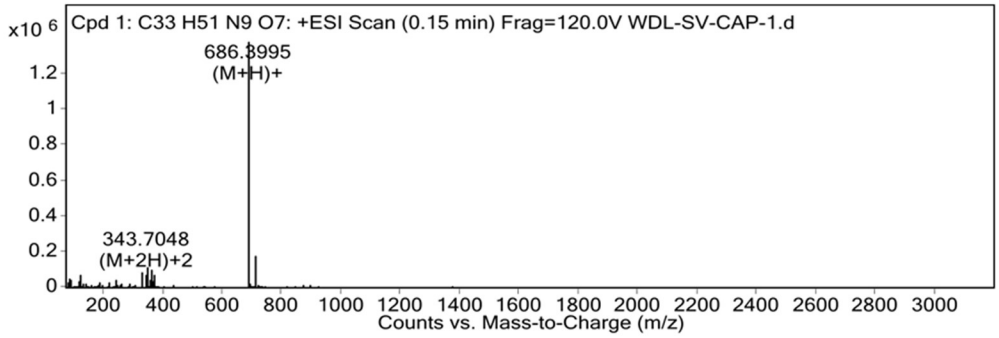

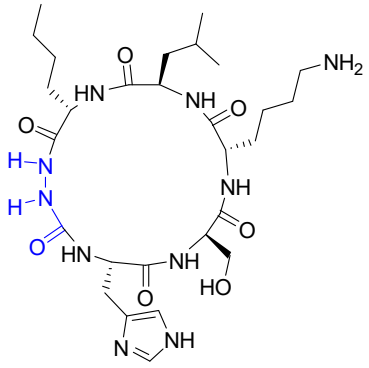

[azaG^4]-CP-2

2.4

a) Method F

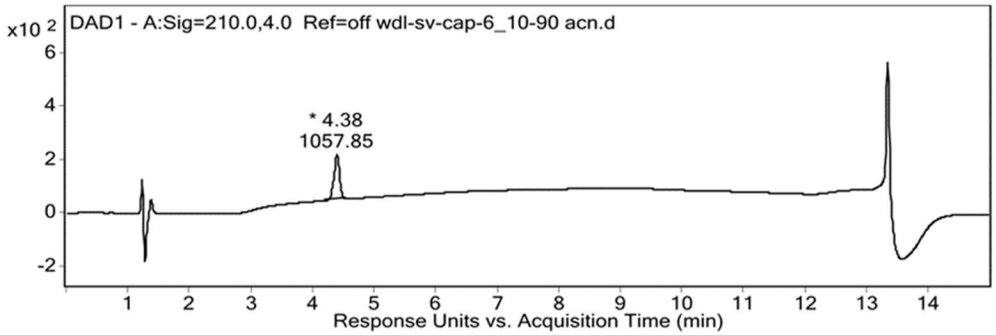

b) Method E

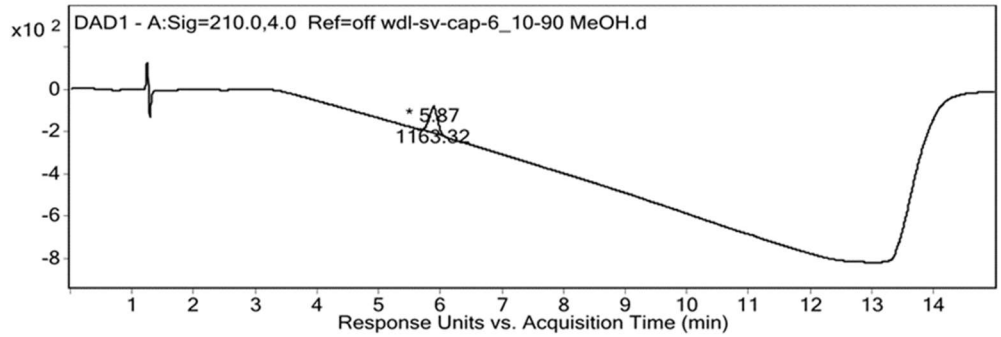

c) HRMS

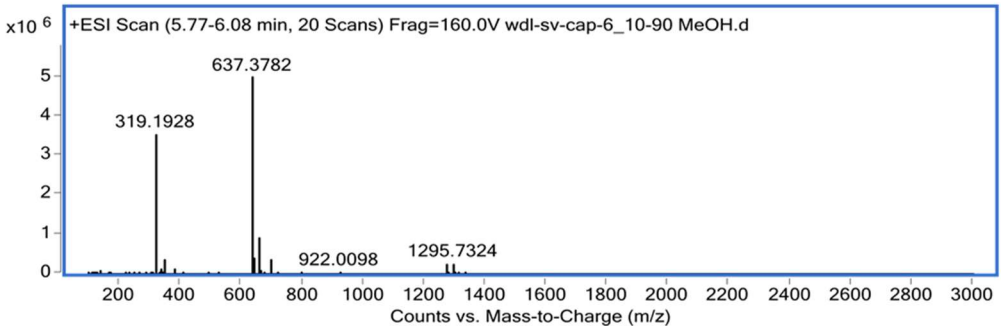

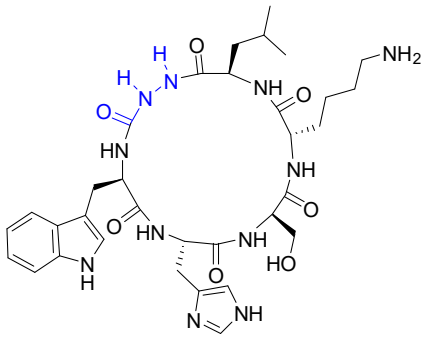

[azaG^5]-CP-2

2.5

a) Method A

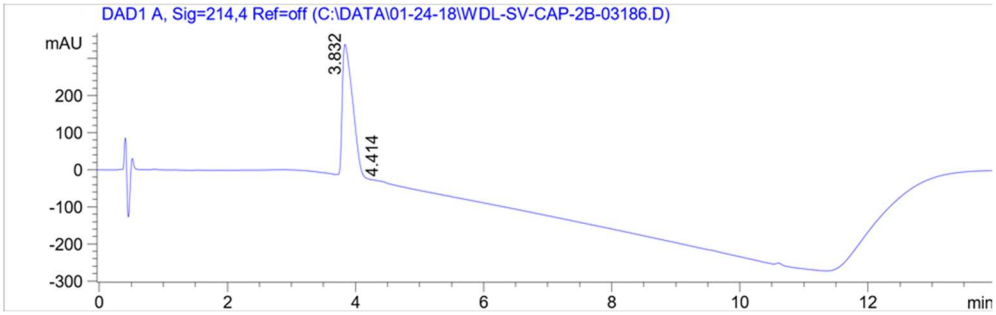

b) Method B

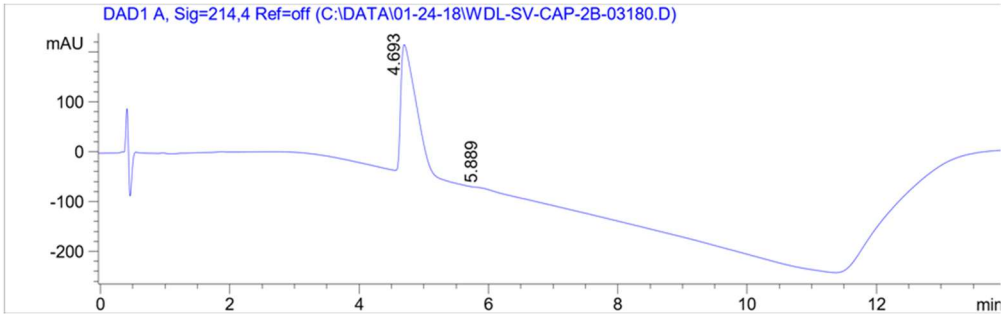

c) HRMS

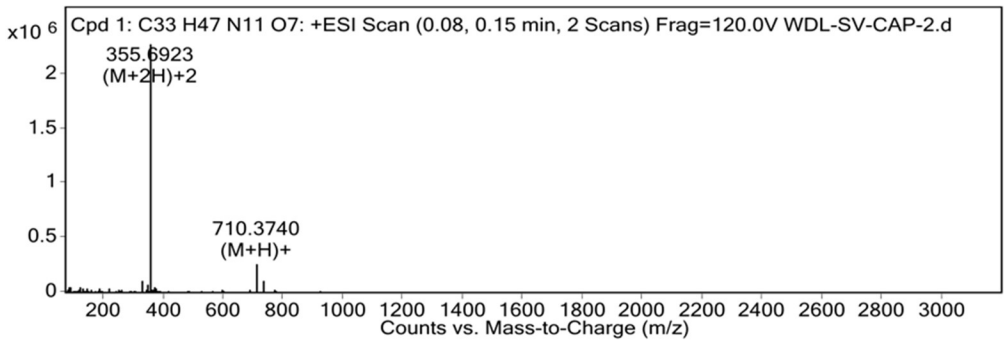

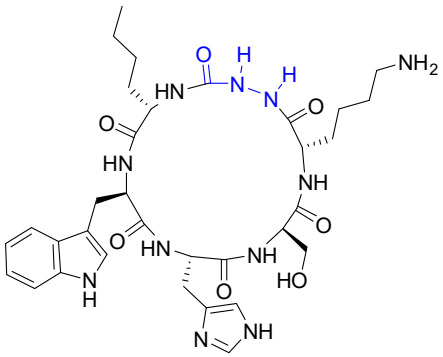

[azaG^6]-CP-2
2.6

a) Method A

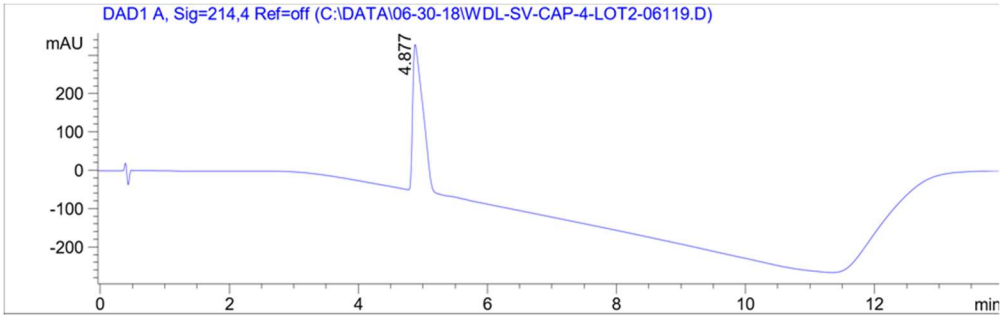

b) Method B

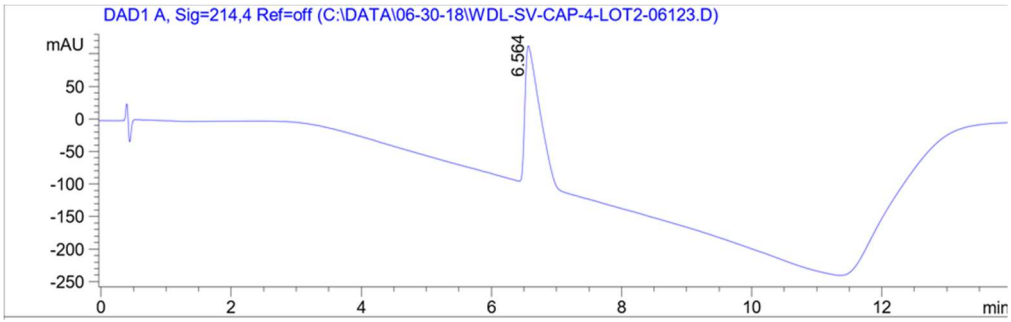

c) HRMS

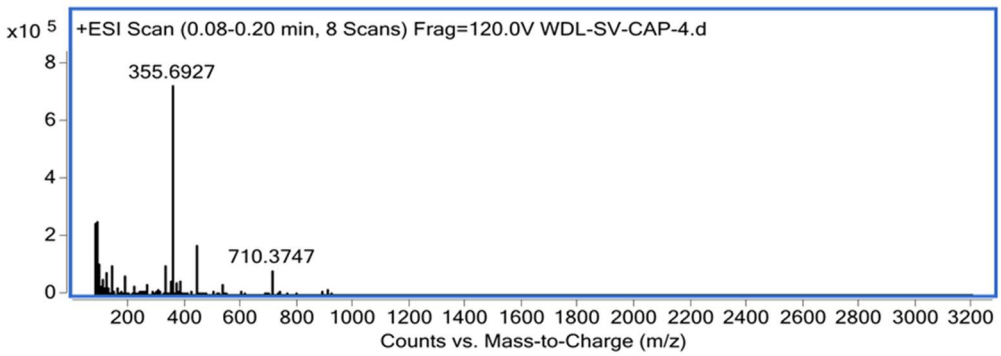

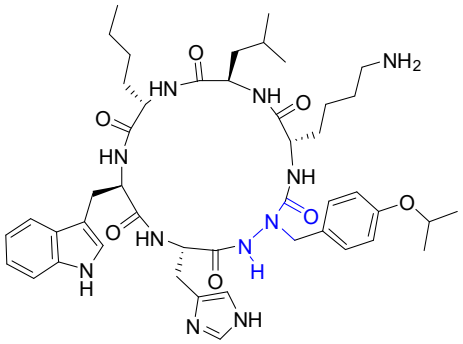

(R)-[aza(*i*-PrO)F^2]-CP-2;
(R)-2.32

a) Method A

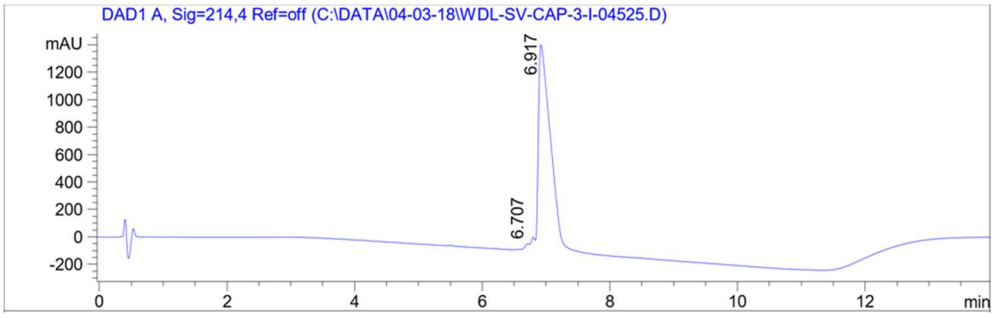

b) Method C

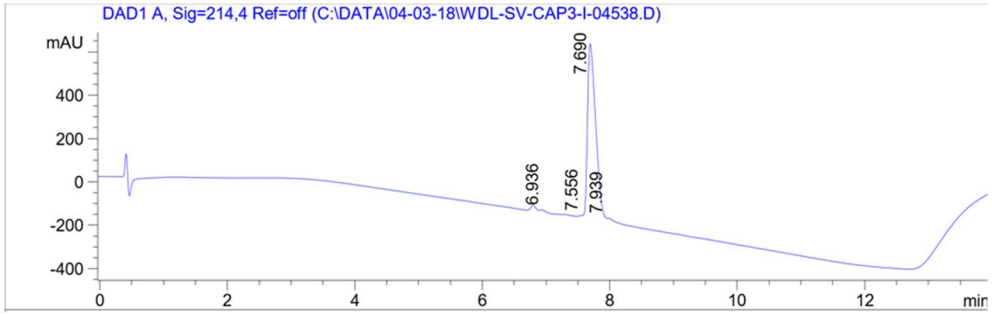

c) HRMS

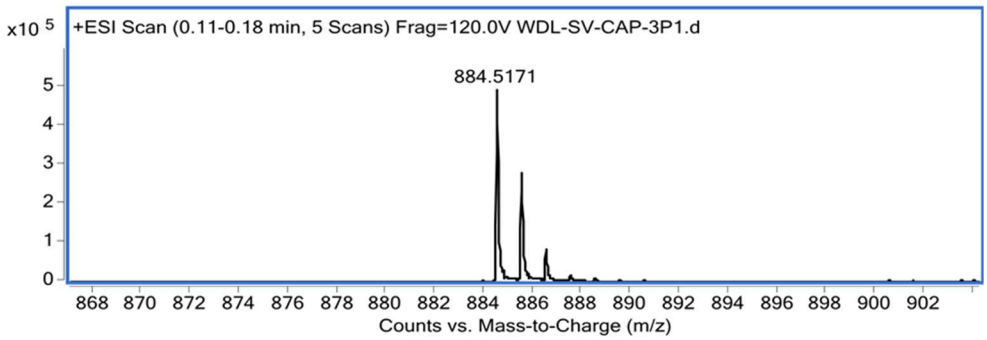

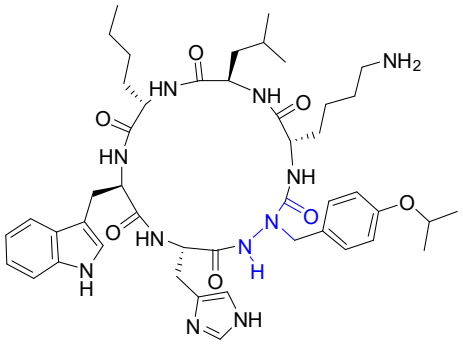

(S)-[aza(*i*-PrO)F^2]-CP-2;
(S)-2.32

a) Method A

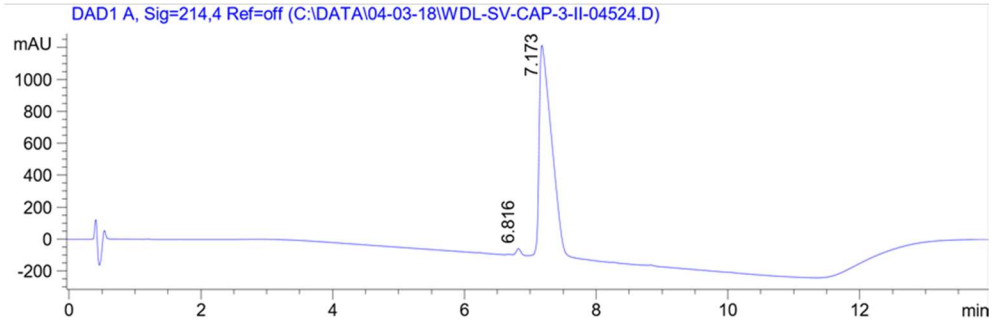

b) Method C

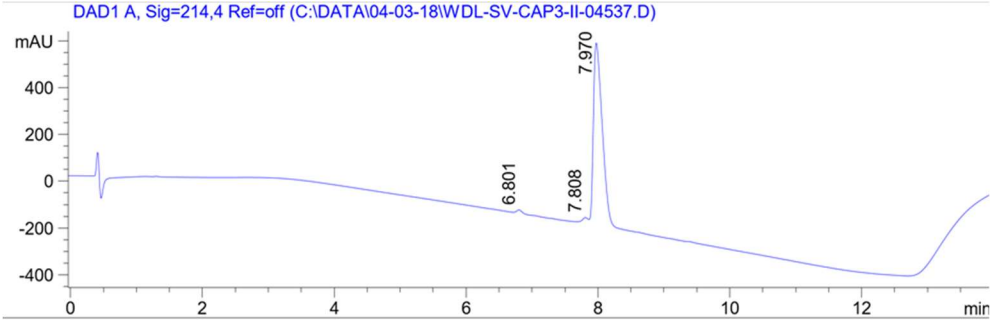

c) HRMS

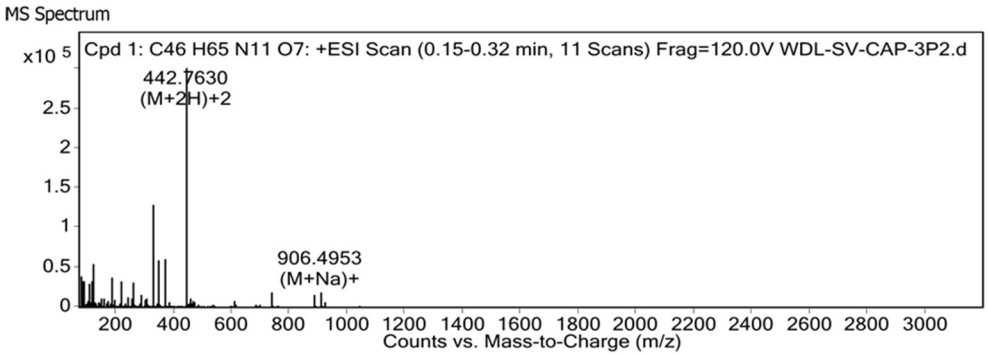

Annex 3: NMR spectra for Chapter 2

^{1}H NMR, 400MHz

Solvent: DMSO-*d*6

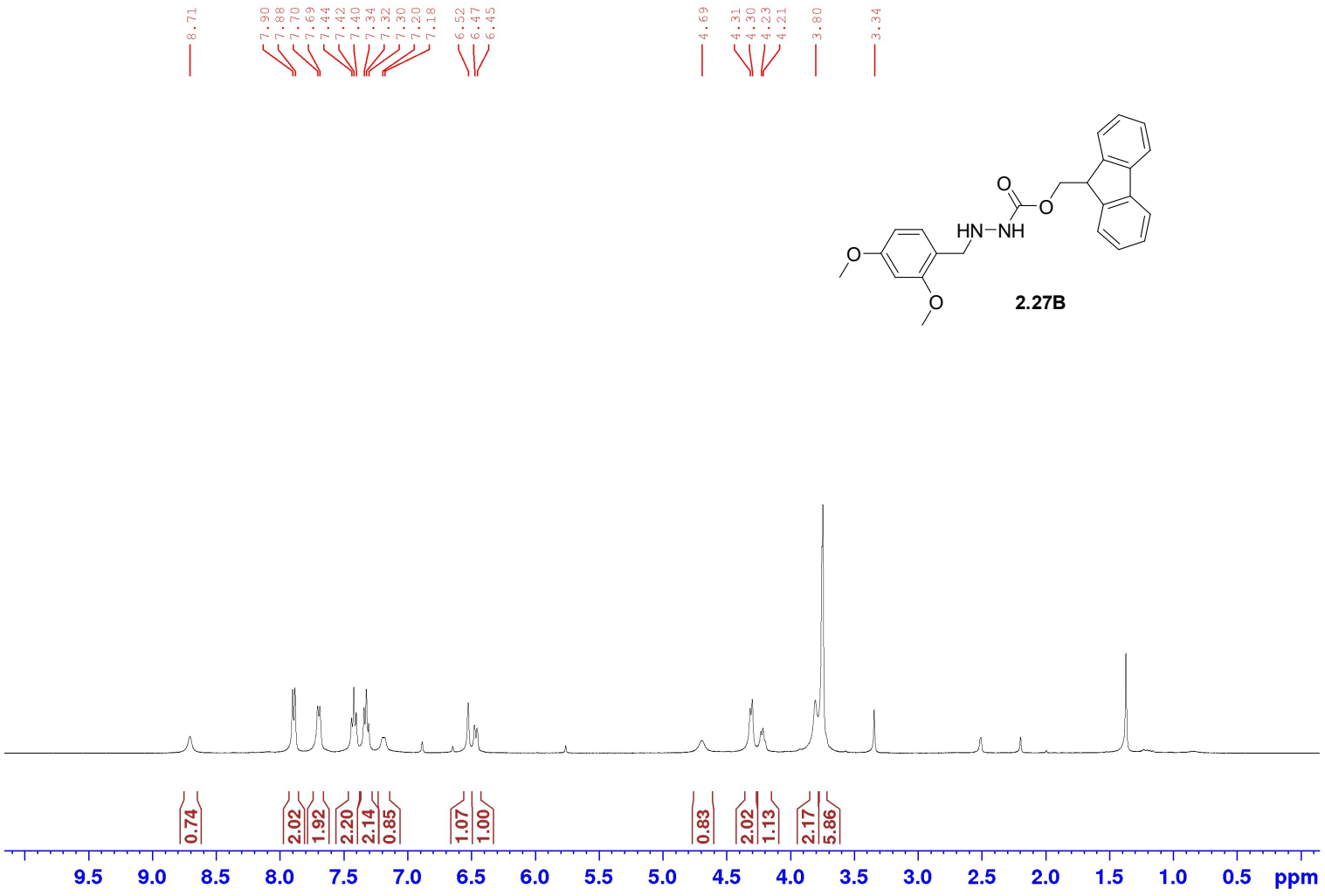

^{13}C NMR, 100MHz

Solvent: DMSO-*d*6

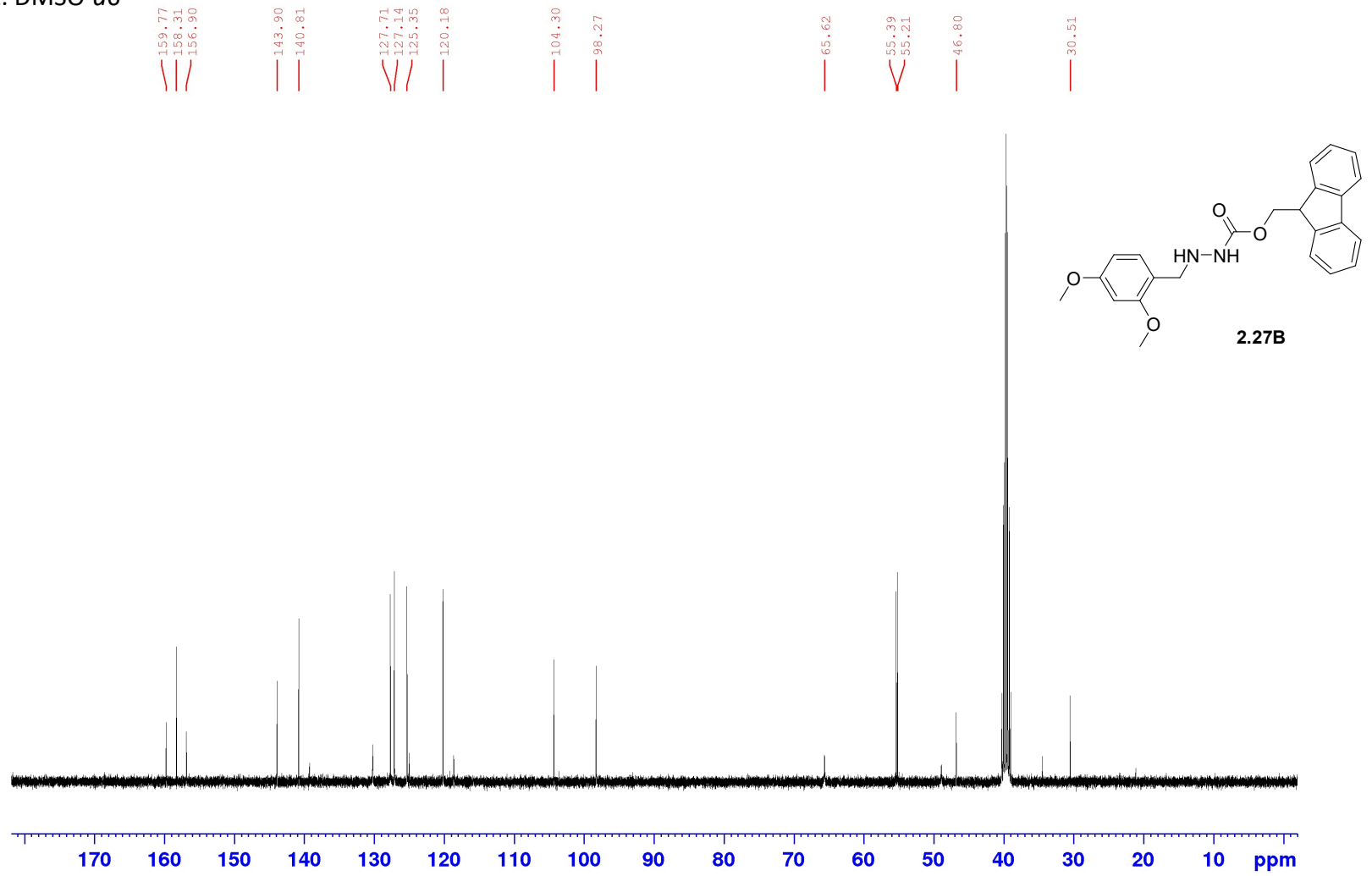

^{1}H NMR, 400MHz

Solvent: DMSO-*d*6

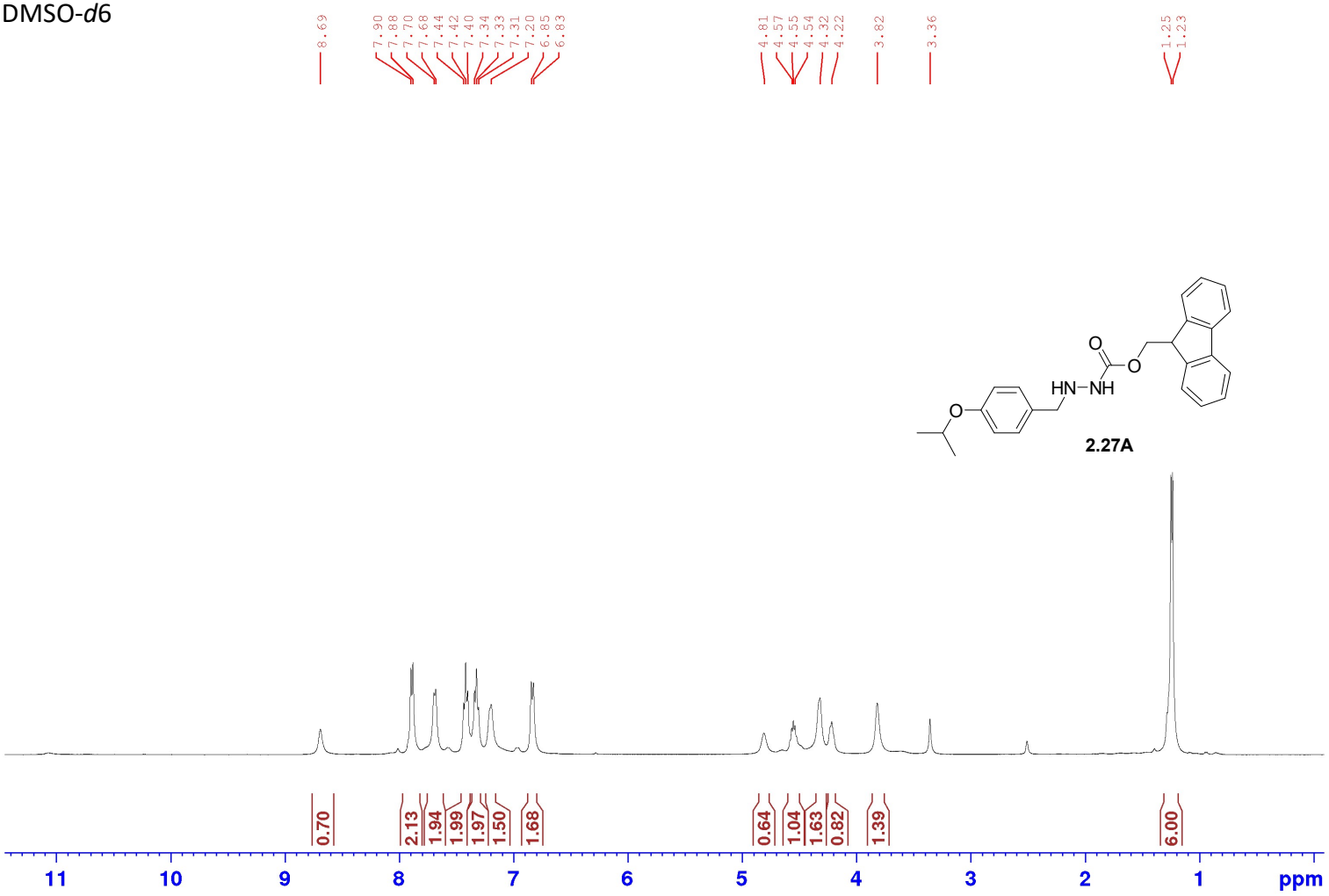

^{13}C NMR, 100MHz

Solvent: DMSO-*d*6

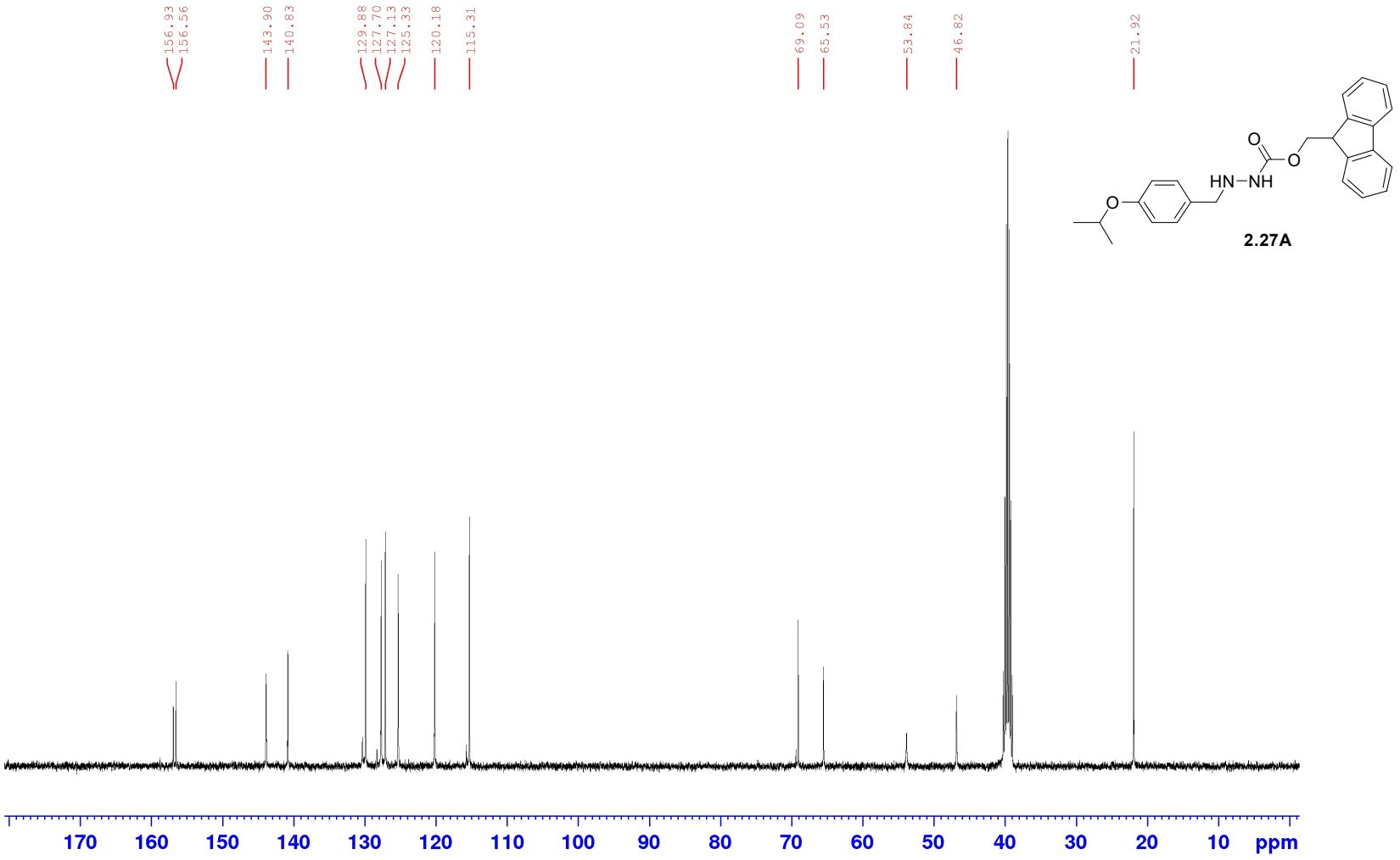

^{1}H NMR spectrum of impurity (27)

^{1}H NMR, 400MHz

Solvent: DMSO-*d*6

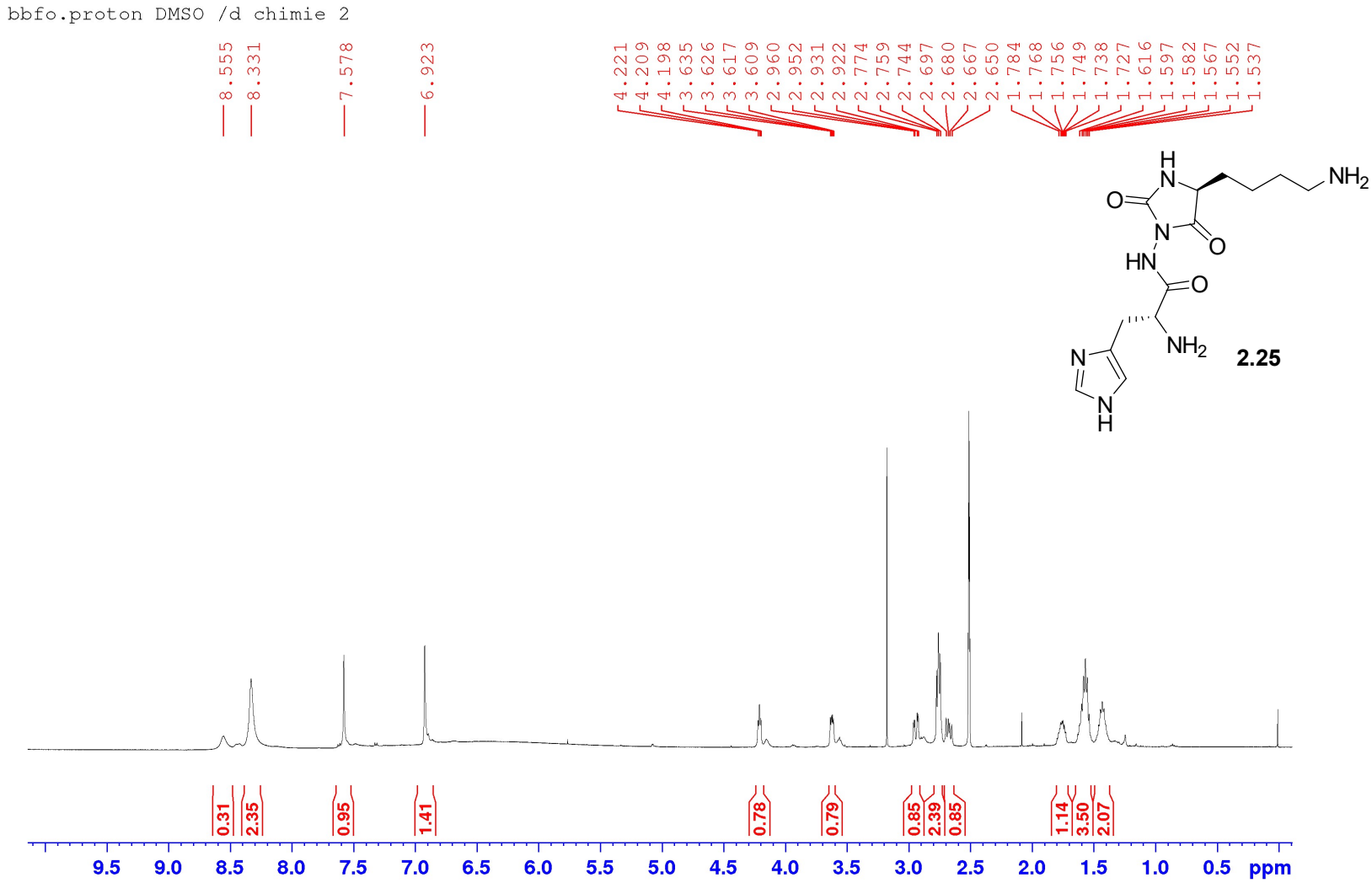

^{13}C NMR spectrum of impurity (27)

^{13}C NMR, 100MHz

Solvent: DMSO-*d*6